



# Performance Study of Darrieus Turbine Using Numerical Simulation

Submitted to the Graduate School of Natural and Applied Sciences  
in partial fulfillment of the requirements for the degree of  
MASTER of Science  
in Energy Engineering

By  
Abdelrahman ABUALEENEIN  
ORCID 0000-0002-1022-7458

February 2024

This is to certify that we have read the thesis **Performance Study of Darrieus Turbine Using Numerical Simulation** submitted by **ABDELRAHMAN ABUALEENEIN**, and it has been judged to be successful, in scope and in quality, at the defense exam and accepted by our jury as a MASTER'S THESIS.

APPROVED BY:

**Advisor:** **Doç. Dr. Ziya Haktan Karadeniz**  
İzmir Yüksek Teknoloji Enstitüsü

**Committee Members:**

**Doç. Dr. Sercan Acarer**  
İzmir Kâtip Çelebi Üniversitesi

**Prof. Dr. Prof. Dr. Alpaslan Turgut**  
Dokuz Eylül Üniversitesi

**Date of Defense: February 06, 2024**

# Declaration of Authorship

I, **ABDELRAHMAN ABUALEENEIN**, declare that this thesis titled **Performance Study of Darrieus Turbine Using Numerical Simulation** and the work presented in it are my own. I confirm that:

- This work was done wholly or mainly while in candidature for the Master's degree at this university.
- Where any part of this thesis has previously been submitted for a degree or any other qualification at this university or any other institution, this has been clearly stated.
- Where I have consulted the published work of others, this is always clearly attributed.
- Where I have quoted from the work of others, the source is always given. This thesis is entirely my own work, with the exception of such quotations.
- I have acknowledged all major sources of assistance.
- Where the thesis is based on work done by myself jointly with others, I have made clear exactly what was done by others and what I have contributed myself.

Date: February 06, 2024

---

# Performance Study of Darrieus Turbine Using Numerical Simulation

## Abstract

In this study, CFD abilities to handle Darrieus turbine simulation were assessed and validated in light of related experimental and numerical studies. Simulation methodology is based on two-dimensional modeling of a double NACA 0018 bladed, straight blade Darrieus turbine. Modeling approach, meshing procedure, and solution parameters are mentioned and discussed in details. ANSYS fluent 18.2 is used to carry out all simulations. Experimental test's data from literature [11] are implemented in context of results verification, also, Courant number and y plus analyses were provided. Due to the simplified assumptions inherent in 2D modeling approximation, a discrepancy of results overestimation was noticed, however the trend of numerical results is close to the experimental one. The aim of this study is to discover the ability of 2D simulation to handle Darrieus turbine power production expectation, and its behavior in case of pair of turbines with a close proximity. CFD results were affected with problem's physics, such that better numerical results were achieved comparing to the experimental results at higher TSR region, where dynamic stall effect is less significant. In this study, we investigated also the possibility of power augmentation for a pair of Darrieus turbines in close proximity. Numerical results have showed enhancements on the average power coefficient of pair of turbines at TSR of 3.5, however, a limited decrease in power coefficient of pair configurations was detected at lower TSRs region.

**Keywords:** Renewable energy, Wind energy, Vertical Axis wind turbine, Darrieus turbine, CFD, pair of turbines.

# Sayısal Simülasyonla Darrieus Türbini Performans Analizi

## ÖZ

Bu çalışmada, Darrieus türbin simülasyonunu işleme yetenekleri, ilgili deneysel ve sayısal çalışmaların ışığı altında değerlendirilmiş ve doğrulanmıştır. Simülasyon metodolojisi, çift NACA 0018 kanat profiline sahip düz bıçaklı Darrieus türbini için iki boyutlu modelleme temellidir. Modelleme yaklaşımı, örgü oluşturma prosedürü ve çözüm parametreleri ayrıntılı olarak belirtilmiş ve tartışılmıştır. Tüm simülasyonlar için ANSYS Fluent 18.2 kullanılmıştır. Literatürden deneysel test verileri [11], sonuçların doğrulanması bağlamında uygulanmış; Courant sayısı ve y artı analizleri sunulmuştur. 2 Boyutlu modelleme yaklaşımının basitleştirilmiş varsayımlarından kaynaklanan sonuçların abartılı tahmin uyumsuzluğu belirlenmiştir. Bu çalışmanın amacı, Darrieus türbin güç üretim beklentisini ele alabilme yeteneğini keşfetmek ve kanatları birbirine yakın olan iki türbinin davranışını belirlemek ve kanıtlamaktır. Computational Fluid Dynamics (CFD) sonuçları, fiziksel problemler nedeniyle etkilendi, bu durumda deneysel sonuçlarla karşılaştırıldığında daha iyi sayısal sonuçlara ulaşıldı. Bu durum, dinamik stall etkisinin daha az belirgin olduğu daha yüksek TSR (Tıbbi Yatırım Oranı) bölgesinde ortaya çıkmaktadır. Bu çalışmada, birbirine yakın konumlanmış bir çift Darrieus türbini için güç artırımının olasılığını araştırdık. Sayısal sonuçlar, TSR'de türbin çiftinin ortalama güç katsayısında 3,5 artış olduğunu göstermiştir, ancak daha düşük TSR bölgelerinde çift güç katsayısında sınırlı bir azalma tespit edilmiştir.

**Anahtar Kelimeler:** Yenilenebilir enerji, Rüzgar enerjisi, Dikey Eksenli rüzgar türbini, Darrieus türbini, CFD, Türbin çifti.

## *Dedication*

*I wish to express my deep appreciation and gratitude to my research supervisor, Doç. Dr. Ziya Haktan Karadeniz, for his leadership, knowledge, and support throughout this exciting course of study. Your passion for research is contagious and you have made my master's program a memorable experience. I would also like to thank my laboratory colleague Ufuk Akgul for all of his support and critical feedback throughout my master's dissertation. As well, I would like to extend my sincerest thanks to Doç. Dr. Sercan Acarer, for taking time out of a busy schedule to provide valuable advices and support for this work. I would like also to thank Prof. Mehmet Çevik for his great support and advices.*

..

# Table of Content

<b>Declaration of Authorship</b> .....	<b>ii</b>
<b>Abstract</b> .....	<b>iii</b>
<b>Öz</b> .....	<b>iv</b>
<b>Dedication</b> .....	<b>v</b>
<b>List of Figures</b> .....	<b>viii</b>
<b>List of Tables</b> .....	<b>x</b>
<b>List of Abbreviations</b> .....	<b>xi</b>
<b>List of Symbols</b> .....	<b>xiii</b>
<b>1 Introduction</b> .....	<b>1</b>
1.1 Overview .....	1
1.2 History and Development .....	7
1.3 Structural Design.....	9
1.4 Aerodynamics Design .....	15
1.5 Thesis overview .....	20
<b>2 Literature Review</b> .....	<b>22</b>
<b>3 Methodology</b> .....	<b>29</b>
3.1 Introduction.....	29
3.2 Darrieus Turbine Analysis Methods.....	31
3.3 Current Model.....	41
3.4 Solution-Grid Independency Check .....	49
3.5 Convergence Criteria.....	54
3.6 Courant Number Analysis .....	55
3.7 Comparison with Experiment .....	57
3.8 Conclusion .....	58

<b>4 Results and discussion</b> .....	<b>59</b>
4.1 Standalone Darrieus turbine.....	59
4.2 Pair of turbines .....	61
4.3 Conclusion .....	67
<b>References</b> .....	<b>69</b>
<b>Curriculum vitae</b> .....	<b>76</b>



# List of Figures

Figure 1.1	Installed wind energy capacity over the world.....	2
Figure 1.2	HAWT and VAWT configurations .....	3
Figure 1.3	Visual illustration for drag and lift forces.....	4
Figure 1.4	Example wind turbine designs .....	4
Figure 1.5	Straight blade Darrieus turbine .....	7
Figure 1.6	Darrieus turbine common types .....	10
Figure 1.7	Power coefficient vs TSR at different number of blades .....	12
Figure 1.8	Typical airfoil profiles used in Darrieus turbine .....	13
Figure 1.9	Schematic diagram for forces act on Darrieus turbines' blade.....	16
Figure 1.10	Angle of attack variation.....	18
Figure 1.11	Counter rotating pairs of turbines .....	20
Figure 3.1	Velocity variation through Darrieus turbine .....	29
Figure 3.2	Prism layers depiction .....	38
Figure 3.3	Experimental apparatus .....	42
Figure 3.4	Actual Turbine's geometry .....	43
Figure 3.5	Computational domain .....	44
Figure 3.6	Mesh structure.....	46
Figure 3.7	Typical $C_p$ vs TSR .....	50
Figure 3.8	Moment production plot for all grids at different TSRs.....	52
Figure 3.9	$C_p$ versus number of elements at different TSRs .....	53
Figure 3.10	$C_p$ variations through rotation progress at TSR 3.0 .....	54
Figure 3.11	Moment curve for subsequent cycles.....	55
Figure 3.12	Clarification of courant number .....	56
Figure 3.13	Courant number distribution for different azimuthal angles .....	57
Figure 3.14	Comparison between numerical and experimental results .....	57

Figure 4.1	Numerical vs experimental results for single turbine .....	59
Figure 4.2	$C_p$ vs TSR, results by F Balduzzi et. al. [15] .....	60
Figure 4.3	Single and pair of Darrieus turbines configurations .....	61
Figure 4.4	Counter rotating, upwind pair configuration .....	62
Figure 4.5	Numerical results for single and pair of turbines.....	63
Figure 4.6	Numerical results for single and pair of turbines by [21] .....	64
Figure 4.7	Average moment coefficient vs $\Theta$ for pair at 1.2D distance .....	65
Figure 4.8	Moment coefficient vs $\Theta$ for pair and stand-alone turbines .....	65
Figure 4.9	Moment coefficient for pair's elements at TSR 3.5 & 1.2D .....	66
Figure 4.10	(a): Wind flow over airfoil, (b) Wake field of a Darrieus turbine .....	67

# List of Tables

Table 3.1	Scales of main analysis parameters .....	33
Table 3.2	Main experimental parameters .....	42
Table 3.3	Domain dimensions relative to rotor diameter .....	45
Table 3.4	Grids details .....	47

# List of Abbreviations

CFD	Computational Fluid Dynamics
GW	Giga Watt
HAWT	Horizontal Axis Wind Turbine
WECS	Wind Energy Conversion System
VAWT	Vertical Axis Wind Turbine
DT	Darrieus Turbine
DOE	US Department of Energy
ALCOA	Aluminum Company of America
SNL	SANDIA National Lab
TSR	Tip Speed Ratio
EEM	Equivalent Electrical Model
DMST	Double Multiple Stream Tube
VTM	Vorticity Transport Model

2D	Two Dimensional
3D	Three Dimensional
N-S	Navier-Stokes
RANS	Reynolds Averaged Navier-Stokes
CFL	Courant-Friedrichs-Lewy
SST	Shear Stress Transport

# List of Symbols

$\rho$	Density [kg/m <sup>3</sup> ]
$\sigma$	Solidity [-]
$\omega$	Rotational speed [rad/s]
$v_\infty$	Wind free stream velocity [m/s]
$c$	Blade's chord [m]
$R$	Turbine's radius [m]
$N$	Number of blades [-]
$V$	Fluid velocity [m/s]
$l_0$	Reference length [m]
$\mu$	Dynamic viscosity [N·s/m <sup>2</sup> ]
$D$	Diameter [m]
$F_L$	Lift force [N]
$F_D$	Drag force [N]

$\square_n$	Normal force [N]
$\square_t$	Tangential force [N]
$F$	Blade's resultant force [N]
$W$	Relative velocity [m/s]
$\Theta$	Azimuthal angle of the blade [deg]
$\alpha$	Angle of attack [deg]
$p$	Pressure [Pa]
$g$	Gravity force [N]
$\square$	Velocity vector [m/s]
$\square'$	Fluctuating velocity component
$t$	Time [s]
$\square_t$	Eddy viscosity []
$Y^+$	Y plus [-]
$\square$	Kinematic viscosity [ $\square^2/\square$ ]
$\square_c$	Friction velocity [m/s]
$\square_R$	Diameter of rotating region [m]

Time step [s]

Cell size [m]

Power factor [-]

*swept* Turbine's swept area

*avg* Average torque production [N.m]

Courant number [-]



# Chapter 1

## Introduction

### 1.1 Overview

Due to the huge and increasing demand on energy supplies, attached with the fossil fuels negative effects on economy and climate, researches in renewable energy technologies improvement have attracted more attention in the last few decades. The urgent need to protect the environment, as well as the infinite utilizable renewable energy resources availability, encouraged the research efforts in all renewables including diverse variety of systems and technologies.

Research on renewable energy aims mainly to find clean, economic, sustainable, safe and local energy supplies. Wind energy represents an ideal option that complies with all those measures well. Wind power has become a key and reliable renewable energy source due to the consistent development and improvements on wind energy conversion systems, reaching up to multiple megawatts of electricity production from a single turbine. Wind energy's total installed capacity has reached 3068.3 GW worldwide as of 2021 [1]. Moreover, wind industry has witnessed rapid growth in the last decades motivated by the recent development in materials engineering, which allowed the manufacture of more reliable material solutions that helped to produce larger and more reliable turbines. Figure 1.1 below shows growth in wind energy utilization worldwide in the last decade.

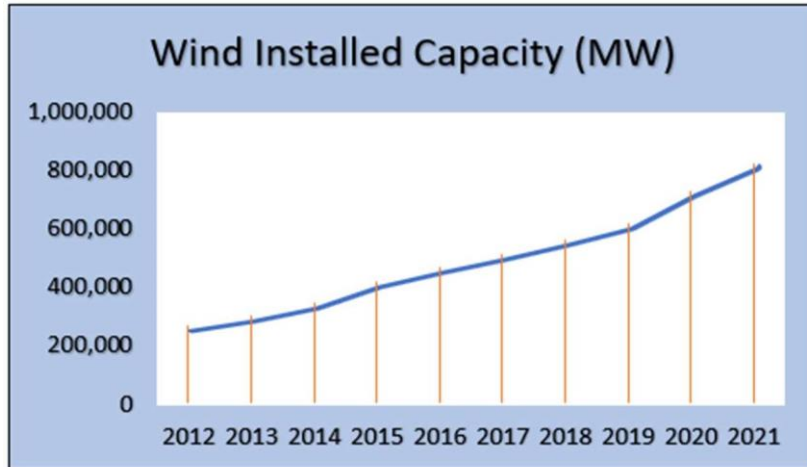


Figure 1.1: Installed Wind Energy Capacity over the World, data from [1]

Wind energy is a form of mechanical energy that is converted directly to another mechanical energy form as a rotational power in generator's shaft, which is in turn converted to electricity. Such advantage of wind energy outweighs many other renewable options, which are based on converting energy from heat or chemical forms into a mechanical energy in order of electricity generation, since that implies conversion losses between different energy forms. This important and fundamental difference between wind and other renewables makes wind systems simpler in principle, and more efficient compared to other renewable systems.

Currently, the most common type of wind turbine is called horizontal axis wind turbine (HAWT) which is shown in figure 1.2 - a. This type has a wider spread than any other wind energy conversion system (WECS), moreover, it has the largest share in research streams and commercial projects. HAWT has many advantages that are thought to outweigh other types of wind turbines. Technically, HAWT is featured with high relative efficiency, proven reliability, and it can be manufactured in scales of Megawatts per unit turbine. Another important reason for HAWT's widespread and popularity, is its history of commercial success which attracted investors to develop and improve better HAWTs. However, new challenges are appearing in the wind energy market that may affect the percentage of HAWT dominance, in the favor of its competitor's namely; the Vertical Axis Wind Turbine (VAWT). Both systems convert wind's motion energy into

shaft rotation in order to produce electricity, but with different mechanisms, structures, and aerodynamics. Figure 1.2 below shows both types.

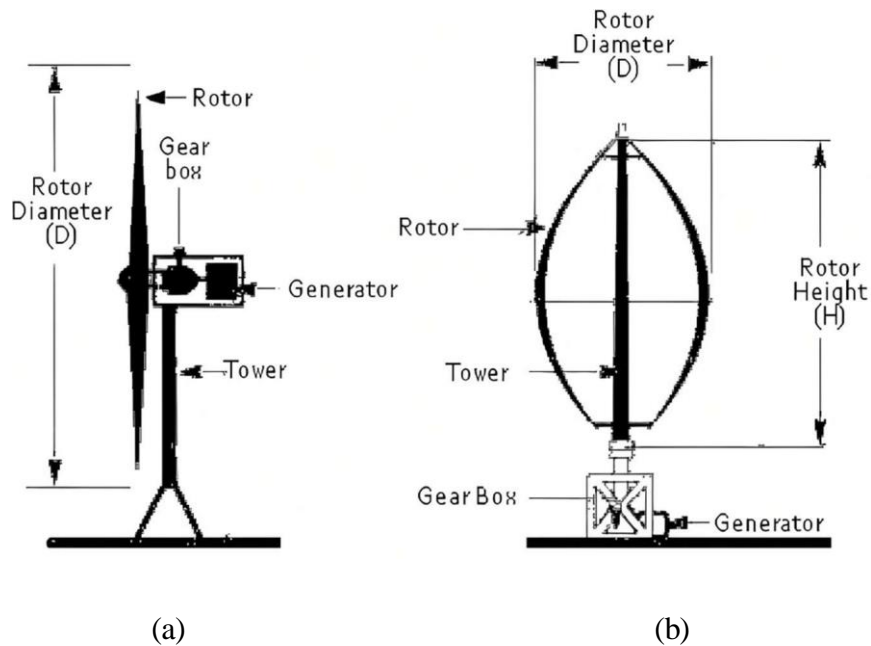


Figure 1.2: Wind turbines types, HAWT (a), and VAWT (b)

### 1.1.1 Working Principle

Wind machines are divided into two types regarding the driving force; lift, and drag machines. In lift devices, the lift force, which is generated by airfoil's profile is doing the useful work. On the other hand, in drag devices, the useful work is produced by the drag force, which results by wind flow against blades. Drag force acts in the same direction of wind incidence upon the blade, as a result of blade's resistance to wind flow. While lift force is produced due to airfoil's aerodynamic lift effect, and acts in a perpendicular direction to wind incidence direction, figure 1.3 below depicts both cases. Due to the principal differences between lift and drag machines, different aerodynamic analysis is applied to each one, and different efficiency limits are expected by each. For lift devices, "Betz's limit" sets 59.3% as the higher efficiency can be achieved - theoretically- by lift machine, whereas the maximum theoretical efficiency for the drag-based turbines is limited to 29.6 % [2].

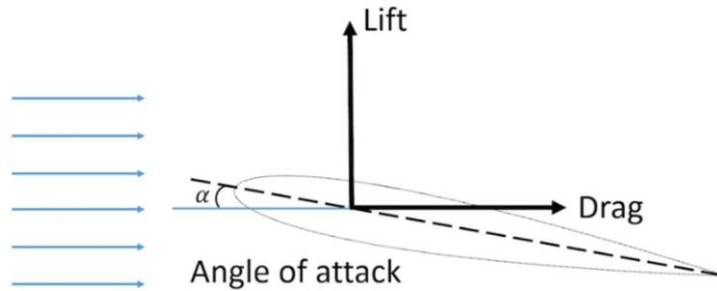


Figure 1.3: Visual Illustration for Drag and Lift Forces.

Both VAWTs and HAWTs can be designed to work as lift or drag devices, examples are shown in Figure 1.4. Although the attended higher efficiency of lift devices makes it more preferred choice, still there is a space for drag devices, especially in small scale applications like pumping water, due to its simplicity of manufacturing and lower costs. Meanwhile, there are hybrid designs for devices that try to get the benefits of both lift and drag forces, such as the Darrieus-Savonius rotor, which is supposed to have better self-starting behavior than a mere Darrieus turbine (lift machine) as-well, better efficiency than a mere Savonius turbine (drag machine). Historically, only drag devices were implemented for applications such as grinding and water transmission, which can be referred to its easier manufacturing requirements as well simpler working principle.

	HAWT	VAWT
Lift Type		
Drag Type		

Figure 1.4: Examples of Wind Turbine designs

### 1.1.2 Importance of Darrieus turbine

Even the HAWT type is considered usually as a more efficient solution for wind energy conversion, due to its good reputation in market through wind turbines candidates, recent studies showed that the VAWT type can be implemented with much better ground area utilization efficiency [3]. Installing a wind turbine farm in certain location limits most other urban activities within its region, in addition to a significant noise production, thus implies limitation on ground areas availability for wind energy projects. So economical ground area utilization becomes a critical factor in achieving goals to increase wind energy share in electricity production up to the desired amount. In HAWT farms, far separation distances are required between each turbine and its neighbors in the same row, also between subsequent rows in the streamwise direction. Meyers [4] showed that a distance of  $10 D$  between HAWTs resulted in a power reduction of 40% compared to similar turbine performance in the freestream, so larger distances are required to insure proper turbine efficiency. In contrast, Darrieus turbine which is the most common VAWT, showed the ability to have even better efficiency when rotating in pairs with close proximity, or in farms with just a relatively small distance between turbines less than rotor's diameter [5].

Onshore wind resources are generally limited to available land resources in windy regions, and can be infeasible to utilize in some cases due to hard terrains or if it is far away distant from power consumers. On the other hand, offshore wind resources appear as a great potential resource that provides solutions for onshore difficulties. Darrieus turbine owns built-in features make it suitable option for offshore operation more than HAWT, like structure stability and ability to work in pairs. Working in pair is important to have zero resultant moment affects basement platform, while the structural stability is referred to the geometrical symmetry around tower which lowers turbines fixing requirements. Another important scope for Darrieus turbine is implementation within urban regions, where decentralized micro generation systems are thought to be useful. Darrieus turbine also has better ability to handle unstructured turbulent flow available in

urban regions with proper efficiency. As a result, Darrieus turbine offers many attractive advantages due to its simple working principle and construction, as listed below:

- Easy to build and maintain as its major parts are located at ground's level including gearbox and generator.
- Owns built-in solutions for main problems facing installing offshore HAWTs, especially cost, maintenance and reliability.
- Efficient land resources utilization.
- Simple structure, easy to manufacture with no tapered or twisted blades.
- Able to work in pairs, with possible advantage of better performance
- Good handling of turbulent unstructured flow, fits well in the built environment.
- Omni-directionality, for standalone turbine case.
- Suitable for small- and large-scale applications.
- Low sound emissions.
- Friendly view, acceptable esthetics.

Despite that all of these points support Darrieus turbine, on the other hand, it has a complex flow field nature, which makes a reliable analysis of mechanical stresses and power production a difficult and challenging task. In addition, blade fatigue issues and torque ripple are an inherent nature of all VAWT turbines, which causes cases of early damage of Darrieus turbine projects before the expected service lifetime ends [6]. However, new technologies of materials manufacturing seem promising to help in providing materials candidates, that can withstand complex stresses and loads effects on Darrieus turbine structure. Also, recently developed analysis methods like CFD are supposed to solve the flow field with more accurate results than earlier methods. To conclude the above discussion, Darrieus turbine can be considered as an advantageous wind energy harvesting machine that needs careful analysis procedure.

Wind stream contains a certain amount of energy that increases with higher wind's speed, this amount can be called the quantity of energy. On the other hand, the “quality” of wind’s energy is related to the structure and regularity of the stream, and it is important in the field of wind energy conversion. Wind stream quality can be defined as a parameter that proportionally related to wind stream smoothness, and inversely related to turbulence level and gusts. While HAWT turbines require a high both quantity and quality wind energy to work feasibly, VAWT turbines have unique features to operate efficiently with lower quality streams. This feature inherits VAWT turbines with a great advantage; since lower quality wind resources are available much more than the higher quality ones.

VAWT turbines is divided into two main subcategories; lift machine like Darrieus turbine, and drag machine like Savonius rotor. Each one is available with multiple designs regarding blade’s shape, number, and some other features. However, for the scope of this text, lift machines namely, the straight bladed Darrieus turbine will be discussed, Figure 1.5 shows an example for tribble bladed straight blades Darrieus turbine.

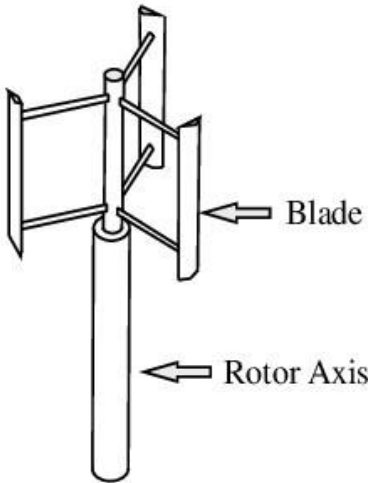


Figure 1.5: Straight Blade Darrieus Turbine

## 1.2 History and Development

Since the 1920s when J. Darrieus has patented his invention, it has presented an interesting research topic and promising source of renewable energy, especially wherever it is expected to fit better than other types of wind turbines. Even though Darrieus turbine is simple in construction, its physics proved itself to be one of the most complex fluid flow cases. Historically, fatigue stresses present the main reason that limited the lifetime of the device below the expectations. Such early failure problems hindered development and spread of Darrieus turbine in past century, but the recent advancement in analysis methods and materials production technologies, is thought to provide efficient solutions. Recently developed materials production technologies is thought to provide better material candidates, that is able to afford high fatigue stresses levels so mitigate a main failure reason in the previous generations of Darrieus turbine, which possibly will give it a chance to be a competitive commercially, and reliable option for long term renewable energy production.

Historically, drag devices were utilized before lift ones due to its simpler mechanism, later in the 19<sup>th</sup> century, the first VAWT for electricity generation was created by James Blyoth [6]. Several decades after that, the French aeronautical engineer Georges Jean Marie Darrieus patented in the year 1926 a new machine to be the first lift driven VAWT device, which called later Darrieus wind turbines. Since invention, Darrieus turbine experienced depleting attention over years, but it became under focus again in the seventies, when oil crisis ignited a huge interest in renewables to be strategic alternative energy resources for fossil fuel.

The first large scale turbine was built by DAF Indal company in Magdalen Islands, Canada with a power capacity of 230 kW, rotor's diameter was 24 m with a cross-sectional area of 595 m<sup>2</sup>, the turbine proved self-starting ability even though it was assumed not capable to do so.



Sandia National Laboratories (SNL) was assigned by the US Department of Energy (DOE) to conduct Research in search of alternative energy resources, including Darrieus turbine. By 1988, a 34 m diameter rotor of phi type rated at 500 kW at 12.5 m/s wind speed was developed in SNL. The power coefficient of the developed turbine has reached a maximum of 0.43 for the struts-less design [6], which presented a high relative value for a Darrieus turbine, while it is typical value for HAWTS.

Successful testing for some prototypes through research centers encouraged some companies to commercialize Darrieus turbine. Aluminum Company of America (ALCOA) served as a blade manufacturer in part of SANDIA projects. Further later, ALCOA has developed its own model of Darrieus turbine called (ALVAWT), with a 17 m diameter, swept area of  $279 \text{ m}^2$ , and expected power production of 100 kW rated at 14 m/s wind speed. This design has reliably operated even under stormy conditions between 1979 and 1981, but the early failure in other projects pushed ALCOA to recall its turbines, leading to the termination of Darrieus turbine development [6].

FloWind company also invested in building Darrieus turbine based on SNL technology in a range of 17 to 19 m diameter of phi design. The turbines have never reached its rated capacity of 300 kW in their operational period and faced early gearbox failure. Moreover, after gearbox replacement with a better model, the rotor failed again due to blade buckling which caused a re-design process to be started in order to enhance the turbine's structure. FloWind has installed and operated over 500 turbines of some successful designs, but later on, Darrieus turbine development was stopped and all FloWind turbines were out of operation by 2004 [6].

### 1.3 Structural Design

Straight blade Darrieus turbine has the advantage of easier manufacturing requirements almost over all other designs, since the blades are just an extruded profile with no twist or taper. However, accurate design procedure is required due to complex loads affecting the turbine while operation.

### 1.3.1 Structure

Darrieus turbines have a main advantage that the drive train including generator and gearbox is situated on the ground, thereby reducing the loads on the tower and facilitating relatively easy maintenance of its systems. Additionally, isolated Darrieus turbine is insensitive to the direction of the wind, and therefore, it does not require a yaw control system. The principal advantage of these features is to enable a design that alleviates the material stress on the tower and require fewer mechanical components. Many designs are available for Darrieus turbines based on the blades shape like phi design, straight blade design, and the helical design, as shown in Figure 1.6. Each design is able optimize certain feature(s) and achieve its benefits; Phi design has advantages of removing the parasitic losses resulted from struts which removes a significant loss. On the other hand, the straight blade Darrieus turbine offers manufacturing ease with its simple blade geometry, and better area to height ratio with relative to curved design. While the helical design goals to mitigate torque ripples which help to lower overall stresses and gain smoother power output with enhanced self-starting ability.

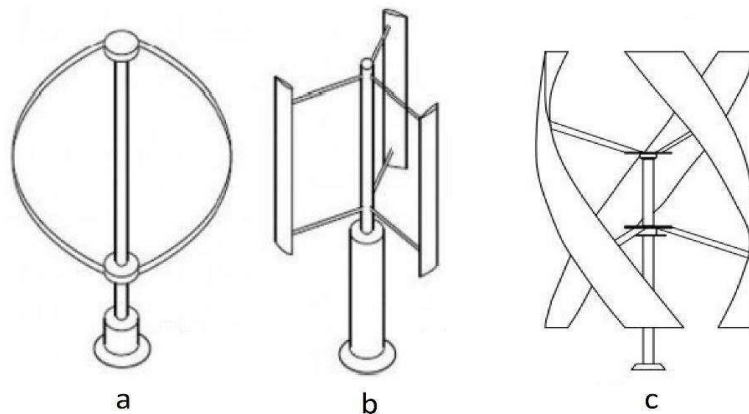


Figure 1.6: Darrieus common designs; (a) phi design, (b) straight blade, (c) helical

### 1.3.2 Design Parameters

Critical parameters that can affect turbine's efficiency significantly are discussed below, in order to show the definition and importance of each one.

### 1.3.2.1 Tip Speed Ratio

Tip speed ratio (TSR) is a quantity represents turbines rotational speed ( $\omega$ ) nondimensionalized with reference to wind free stream speed ( $v_\infty$ ), mathematically shown by the equation 1.1 below:

$$\lambda = \frac{\omega R}{v_\infty} \quad 1.1$$

TSR has a significant effect on turbine's performance presented by a direct proportionality to efficiency from start-up point until reaching an optimum value of TSR, the point at which the efficiency starts to drop with higher TSR, as shown in figure 1.7. Design procedure should ensure turbine's ability to cross through the startup region reaching the optimum region of operation. Dynamic stall is an effect appears strongly in startup region as it reduces rotor's ability to produce power, or even increase its own velocity to reach better operation conditions. Increasing TSR over the optimum region, leads to a reduction of the turbine virtual permeability, making the turbine more and more similar to a bluff body which reduces the flow rate through the turbine and cause performance deterioration.

### 1.3.2.2 Number of Blades

Number of blades is a key parameter that affects Darrieus turbine performance. As the number of blades increases in a certain rotor, its peak value of power production increases too. Figure 1.7 shows power coefficient versus TSR curves for a certain rotor with different numbers of blades from single to five blades; it's clear that increasing the number of blades raises the peak power production significantly until reaching three blades. Increasing the number of blades more than three blades shows no positive effect on peak power production while shortening the peak extent with noticeable deterioration after the peak at higher TSRs, so the most common designs are the two and three blades.

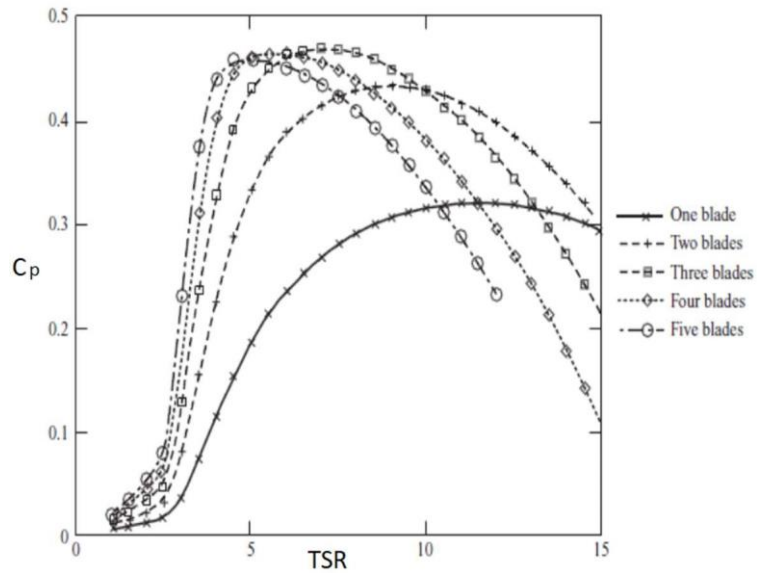


Figure 1.7: Power Coefficient Vs TSR for Different Number of blades [7]

### 1.3.2.3 Blade Profile

Selecting the blade profile affects the turbine performance significantly within both start-up and optimum operation modes. In the case of Darrieus turbine, blades experience continuous variation in all flow characteristics while rotation, such as Reynold's number, relative velocity, and angle of attack. Such oscillation affects negatively on blade's ability to generate lift and produce power. Since blades face both positive angles of attack within the upwind half of turbine, and negative values in the downwind half, symmetric airfoil profiles are commonly preferred in Darrieus turbine to get the advantage of both positive and negative angles of attack in generating lift. While selecting blade's profile, sensitivity of the profile should be checked, as some families of airfoils are sensitive to the roughness, Re, wake, or other parameters. Profile's sensitivity may lead to lose performance significantly, if operational conditions got a deviation from design conditions. Figure 1.8 below shows the typical profiles which are commonly utilized in Darrieus turbine.

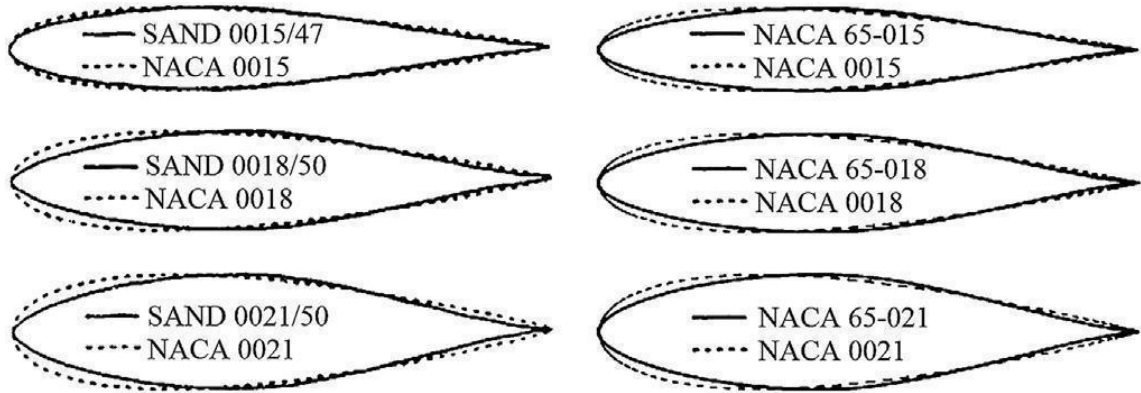


Figure 1.8: Typical Airfoil Profiles Used in Darrieus turbine [8]

### 1.3.2.4 Solidity

Turbine's solidity ( $\sigma$ ) is the ratio of the circumferential distance occupied by blades to the diameter of the rotor, which can indicate how much of the turbine swept area is blocked by blades. Equation 1.2 shows a common mathematical formula for solidity based on the diameter; however, it is worth notifying here that another definition exists in literature based on radius instead diameter. The major effect of solidity increasing is a progressive retardation of the flow in the downstream area, causing the blade's loading unbalance in the upstream and downstream rotor's halves. Increasing solidity causes higher energy to be harvested in the upwind half, while lower energy become available in the downstream for harvesting. However, increasing solidity to certain limit can enhance the overall efficiency, M. Nahas [9] founded that increasing solidity of a certain straight blade Darrieus turbine from 0.06 to 0.14 caused a power coefficient to increase by 22.7%.

$$\sigma = \frac{z * c}{D} \quad 1.2$$

Most of the turbine's power production is extracted in the upwind half, then flow experiences retardation while passing to downstream half. Increasing rotor solidity intensifies flow retardation after the upwind region, so less energy is available and

though can be extracted in the downwind region. On the other hand, Higher solidity Darrieus turbine have generally better self-starting ability due to higher static lift, also, higher power coefficients at lower TSRs are witnessed generally with higher solidities, as depicted previously in figure 1.7.

#### 1.3.2.5 Struts' Profile

Struts are necessary elements in the straight blade Darrieus turbine which connect the tower and blades together; thus, it is responsible for keeping structural integrity, affording stresses like centrifugal stress, and transferring the useful torque from blades to the tower. Even though struts play an important role, its existence creates aerodynamic losses called parasitic load, which lower the overall power yield. For that reason, struts are usually designed with a smooth shape of the cross section like airfoils, taking into account the structural requirements. In the phi type of Darrieus turbine, struts can be removed as done by SNL with a successful design, which achieved significantly higher power coefficient than the struts featured rotor of the same design [6].

### 1.3.3 Failure

Fatigue stresses are generally the main and critical reason for failure in Darrieus turbines, caused due to high loads with alternating nature which induced by the rotating structure. Even though many approaches tried to solve Darrieus turbine flow physics and expect loads accurately, in most cases the results ranged within a low level of accuracy, the fact that clarifies many cases of early failure for Darrieus turbine. While understanding isolated rotors is a research problem, more complexities appear when locating one turbine in another ones' wake, like in case of wind farms, or pairing rotors. Even locating Darrieus turbines close to each other presents an advantage that efficiency may increase, however, still it's important to understand the additional stresses affected by neighbor rotors to ensure the desired lifetime expectations.

Centrifugal stress is a built-in problem in all rotating machines, even though its effects can be mitigated to certain limits by raising the accuracy of manufacturing processes. Hollow blades are used commonly to lower centrifugal stresses, as will overall machine's weight. In addition, aerodynamically-induced stresses can be lowered also by design solutions like helical design. Another useful solution to mitigate critical stresses is blades' "articulation"; which means to keep a small degree of freedom for blades to move or rotate instead of strictly fixing it, this technique is already implemented in helicopters as an example. Articulation helps to mitigate stress effects plus enhance efficiency of Darrieus turbine and self-starting ability [8]. Common modes of Darrieus turbine's failure modes are mentioned below

- Metal fatigue
- Control fault
- Over speed
- Resonance
- Gearbox failure

## 1.4 Aerodynamics Design

The continuous variation in all aerodynamic characteristics for each azimuthal position while blades' rotation, with the absence of any symmetry between upwind or downwind halves, makes Darrieus turbines present a highly complex aerodynamic problem. The complexity of Darrieus turbine physics lies certainly in the unsteadiness, and the interaction between blades with each other and between rotor's upwind and downwind halves, in addition to dynamic stall, and curvature effects. Theoretically; the maximum efficiency of Darrieus turbine of phi type was calculated by Strickland [10] resulting in a power coefficient of 0.48.

## 1.4.1 Blade

Lift and drag forces are produced by airfoil profile due to wind flow upon it, both forces have lines of action depends on the relative velocity direction seen by blade, such that lift force ( $\square_L$ ) is perpendicular to relative velocity direction, while drag force ( $\square_D$ ) acts in the same direction of relative velocity as shown in figure 1.9. Since relative velocity is varying continuously both in direction and magnitude while turbine rotates, in sequence; both drag and lift forces are varying in magnitude and direction. The main driving force of Darrieus turbine is called the tangential force ( $\square_t$ ). Tangential and normal forces are defined with reference to rotation path, so it is more directly related to turbine's operation and easier to be analyzed. Tangential force is a resultant of components summation from lift and drag forces in tangential direction of rotation path, while normal force is resultant of the components perpendicular to the tangent, as clarified in figure 1.9 below.

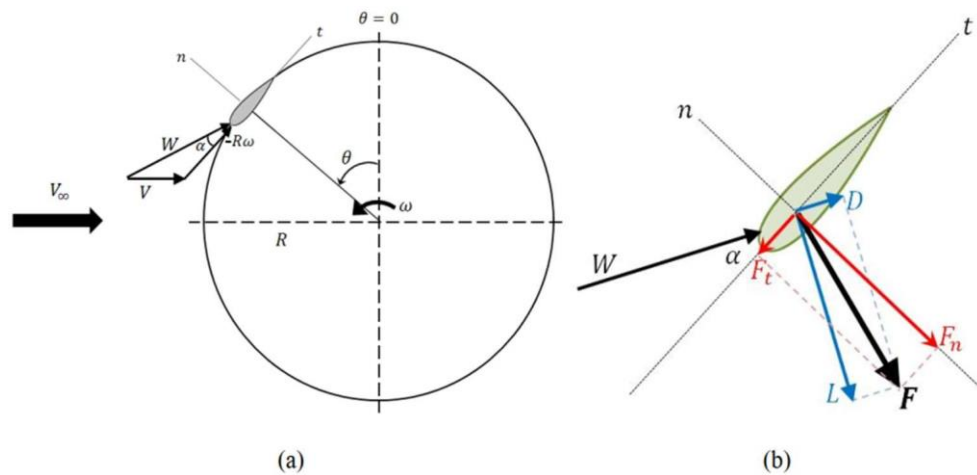


Figure 1.9: Schematic Diagram for Forces on Darrieus turbine's Blade

Due to the rapid oscillation in angle of attack on Darrieus turbine blades, the stall mode of blades is called dynamic stall, which has different behavior than static stall commonly exists in other aerodynamic applications like aircrafts. In the case of dynamic stall, stall is witnessed to start at lower angles of attack. Even though it raises flow complexity, dynamic stall can feature the turbine with an advantage of breaking effect called



aerodynamic breaking, which means that by following a certain design procedure, dynamic stall can be advantageous to get power production regulation at high wind speeds, which can save the device from over speed damage.

## 1.4.2 Self-Starting

One of the major challenges in the Darrieus turbines industry is the self-starting issue. These turbines are claimed to be unable to self-start due to significant dynamic stall effects at low rotational speeds region, so, an auxiliary system is a common option used to accelerate the rotor to its designed operation speed region. Many solutions were offered for start-up issue; such that an improved designs like helical and hybrid Darrieus- Savonius designs, moving to adding a special startup system, increasing the number of blades, or using the variable blade pitch system. Those options were intended to inherit the self-starting ability of Darrieus turbines; however, the added cost and complexity of such solutions was another question. Normally, Darrieus turbine costs include; manufacturing cost, site preparation cost, maintenance cost, and financing cost. Adding an additional cost for a startup system may lower investment feasibility less below other renewable systems candidates. To have a better idea about start up systems, a brief introduction to the common systems is provided below.

### 1.4.2.1 Start-up Motor

One of the common solutions to start a Darrieus turbine is to feed power to the generator, so it acts as a motor while startup until reaching around the optimum speed, then switching it to generation mode. The advantage of this technique is ensuring proper operation of turbine within the optimum speed region. But on the other hand, it costs a significant efficiency drop, since starting up power consumption lowers the overall yield significantly. In addition, the need of special equipment including generator, sensing and control apparatus is also an added cost and complexity to the system.

### 1.4.2.2 Variable Blade Pitch

Opposite to HAWT turbines, Darrieus turbine blades produce a varying amount of torque depending on its azimuthal position. Lift generation by airfoil is related directly to the angle of attack through blade's lift coefficient. The angle of attack ( $\alpha$ ) is defined as the angle between the chord line of the blade and relative velocity vector ( $W$ ). The angle of attack in Darrieus turbine is oscillating between negative and positive values in each cycle as shown in figure 1.10, with amplitude of oscillation depends on TSR. Due to this variation of the angle of attack, torque contribution by the blade is always oscillating between positive and negative values through each revolution for the fixed blades rotors.

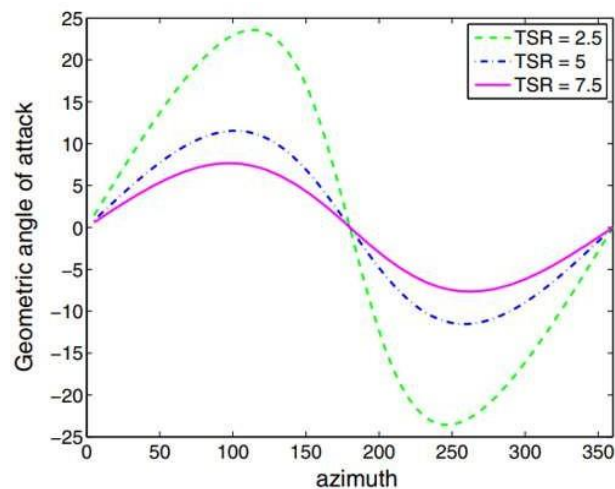


Figure 1.10: Angle of attack variation [10]

As shown in figure 1.10 above, turbine rotation at lower TSR imposes a larger amplitude of variation in angle of attack which amplifies the dynamic stall effects, and so causes performance loss.

Controlling the angle of attack to be within a certain optimum region while blade's rotation, can enhance performance significantly by removing dead regions where the blade produces negative torque. Adding a mechanism to control blade's orientation, instead of fixed blades, is a key feature to enhance the turbine's efficiency by preserving

favorable angles of attack. Such a system is called the variable pitch blade system, and it has many techniques to be applied, like the simple mechanism based on centrifugal force as described by M. Nahas [9], or by an actuator-based systems with more accurate control based on advanced controllers. Due to the added cost and complexity, the variable pitch system is not a common feature of Darrieus turbine.

Both starting-up system and variable blade pitch represent an added cost and complexity to solve the self-starting issue of Darrieus turbine, however, variable pitch still seems more beneficial, as it aims to maximize turbine efficiency in addition to granting the self-starting ability.

### 1.4.3 Pairs and Arrays

Pairing Darrieus turbines has been mentioned in recent studies to enhance power output per unit up to exceed the isolated turbine's efficiency [11]. Such claimed feature of Darrieus turbine presents a key stone to increase the efficiency of the turbine's arrays with more efficient ground area utilization. Moreover, an increase in the efficiency of latter rows can be expected through streamwise direction with relatively small distance between rows, such increase is attributed to flow acceleration while passes between former row's rotors as well as the turbulence level increase which is friendly for Darrieus turbine. Furthermore, pairing Darrieus turbines in an offshore platform cancels resultant torque (fixing torque) of a pair in counter rotating mode, which provide more stability for offshore installation.

Pairing rotors is divided into multiple configurations, downwind (figure 1.11 - a) and upwind (figure 1.11 - b), based on the moving direction of blades in between rotors with respect to wind direction. Another classification for pairs configurations is co-rotating and counter rotating which is based on rotation direction for rotors with respect to each other, figure 1.11 shows counter rotating pairs.

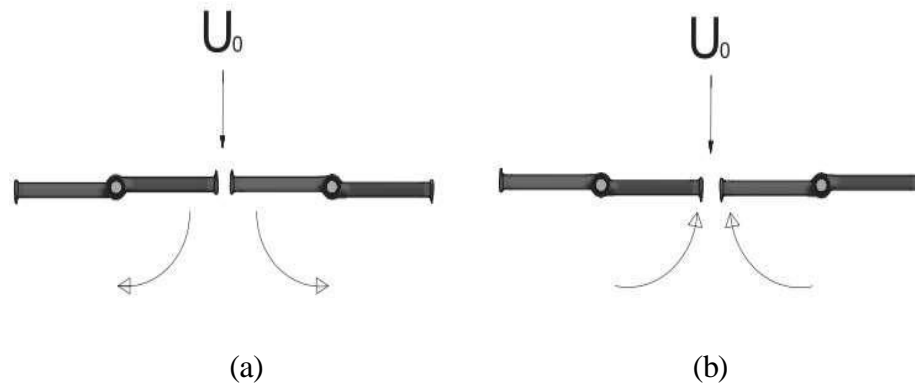


Figure 1.11: Counter rotating pairs of turbines

The standalone Darrieus turbine operates independently of wind direction, such that it can receive wind from all directions without need for a yaw control system. While on the other hand, the pair of turbines' performance depend highly on wind direction due to shadowing effect in case of unfavorable wind flow direction.

Many challenges still hinder Darrieus turbine spread as a proven solution for centralized and decentralized electricity generation. Research efforts are trying to find better approaches to handle the problems in order to optimize better and more reliable design. Overall Performance, and starting-up issue, structure reliability, as well as the control systems present the main parameters for optimization. Many successful prototypes and commercial models already proved Darrieus turbine advantages, but a strong competitor is already taking the largest share in the market. Increasing attention to renewable energy resources supported with new technologies are thought to help in moving forward into manufacturing better generations of Darrieus turbines which are able to work efficiently and everywhere.

## 1.5 Thesis overview

First chapter is dedicated for providing introduction about the case under discussion with a simple sequence of ideas clarifying Darrieus turbine's principle of work, main structural parts, and its prospected advantages. In the second chapter, a quick literature review is presented, starting from the history of Darrieus turbine passing through the important trials to understand, and implement it in the last century reaching current time. Third chapter discusses the methodology we considered to handle the problem of analyzing Darrieus turbine performance, and highlights our procedure in details. Finally, chapter 4 presents the results we achieved, results are discussed in light of experimental results and similar studies achievements.

# Chapter 2

## Literature Review

Global warming and climate change are rising issues worldwide nowadays, which implies reducing carbon dioxide emissions significantly in order to save the Earth's ecological balance. To help in transition from fossil fuels to cleaner energy resources, research efforts aim to develop more efficient renewable energy conversion systems. Withing all kinds of renewables, wind energy presents a vital research topic due to the importance and widespread use of wind turbines worldwide besides the efficiency, feasibility, and reliability proved by the common horizontal axis wind turbines. Currently HAWT is dominating the wind energy industry due to the absence of a strong competitors, however, an escalating interest in research field appeared recently regarding discovering Darrieus turbines' advantages and capabilities. The related published literature indicates a possibility for Darrieus turbine to play a vital role in the future renewables market, specially where its fit better than HAWT.

Most early Darrieus turbine's studies aimed to provide a theoretical approach to estimate its performance characteristics, but rarely experimental data are included as found in references [12,13,14]. The scarcity of laboratory results can be referred to the high cost and complexity of Darrieus turbine experimentation. Because of that, modern numerical methods i.e., Computational Fluid Dynamics (CFD), has become a cornerstone in studying Darrieus turbine performance, augmented with the rapid development in CFD models as well as computational power resources. Many studies have provided CFD simulation results for Darrieus turbines with a good matching compared to experimental and/or analytical results [12,15]. However, still there is no agreed procedure to model and simulate Darrieus turbines in the published literature, and many conflicts appear on the surface between simulation procedures followed in the published articles [16].

The ability to work in close proximity pairs and arrays with a higher possible efficiency, distinguishes Darrieus' machine from the commonly used HAWT machines. Some studies have already shown a significant increase in power production for a pair of turbines compared to the isolated turbine [11,17]. Pair's efficiency enhancement depends on many factors, especially, rotation direction, wind incidence direction, TSR, and the distance between rotors which plays a vital role to determine the overall performance behavior of the turbines' pair, however, there is a lack in studies discussing the effects of those parameter and the mutual interaction effect between them [17]. In context, this work aims to investigate the ability of Darrius turbines pair to enhance or keep a proper efficiency in the case of turbines at close proximity, effect of distance between rotors, and TSR variation, on the overall energy conversion performance will be discussed too.

In his patent in 1926 [18], G. Darrieus has shown suggested designs for a "turbine with a rotating shaft transverse to the flow of the current", which was called later on "Darrieus turbine". Many arrangements were presented in the patent including three and four bladed designs, with both straight and curved blades configuration. Even though the patent came only in four pages, it has ignited further research efforts in thousands of researches. Some of the fundamental turbine's characteristics were mentioned in the patent, like its ability to have a tip speed exceeding the wind speed and the lower rotation resistance than other possible designs. However, the patent contained no theoretical approaches or mathematical relations related to assess the new device performance.

Generally, Darrieus turbine commercial projects experienced an early failure problem through1 the last century as listed in [6], such unsuccessful trials helped HAWT to dominate the market of wind turbines till now. On the other hand, V. Mendes et al [19] state that Darrieus turbine is experiencing a growing interest for development and installation, to be used for decentralizing energy conversion. Darrieus turbine owns advantages like insensitivity to wind direction changes, smaller number of components, lower noise production, better ability to generate energy from irregular wind, easier to

integrate in urban architecture, ability to operate closer to the ground level, and better ground utilization, which can make it a strong candidate in future renewables market.

Kumar et. al. [6] have studied the development of the Darrieus turbine. Different arrangements of the turbine were reviewed regarding performance, blade configuration, tower design, and mode of failure. They stated that early designs mostly failed due to metal fatigue since the composites were not developed yet. But on the other hand, they assured that the Darrieus turbine can provide a solution to the challenges faced by HAWT especially in the offshore environment in terms of reliability, maintenance, and cost. Also, they expected that Darrieus turbine will be a future alternative for wind energy conversion [6].

Three main methods were introduced in literature to analyze Darrieus turbines for performance prediction, analytical approaches, experimentation, and numerical simulation methods. Most studies combined two of the methods mentioned above, like an analytical approach supported by experimental data [19,12], a simulation procedure supported by either experimental [22,15,23], or theoretical findings [20,24]. Despite its small number, experimental studies acted as an important basis for development of theoretical and numerical methods. Most experimental studies were laboratory-based studies using wind tunnel apparatus [11,13], or towing tanks [12]; however, much less number is available for site tests [4,9]. Recently, the numerical simulation method has dominated the research stream of Darrieus turbine studies. Numerical simulation offers lower cost than experiments attached with a good accuracy that can be achieved depending on the followed procedure. In addition to that, it provides the ability to analyze the physical phenomenon's details like flow separation, wake, blades interaction, and stall, which present an attractive feature of simulation. Most numerical simulation studies used to compare the results of simulation with experimentally or analytically produced data, in order to validate the procedure which is also followed in this text. However, another kind of validation can be done also by comparing the simulation results with other numerically produced results [21].



Y. Han et. al. [20] compared different procedures for predicting Darrieus turbine's performance. Three distinct aerodynamic prediction methodologies were implemented and compared to each other. One is a low complexity analysis that is based on the double-multiple stream tube model. The second method was a medium complexity analysis which utilizes a potential flow model based on the velocity field through the near wake region. The last method was a higher complexity analysis of computational fluid dynamics. Two different test cases were studied in order to highlight and specify the prediction capabilities of the three approaches. The results of the aerodynamic loads acting on the rotor blades and whole turbine's power coefficient were obtained by three approaches and then compared with the experimental data. The advantages and disadvantages of each method were discussed in detail.

In their study, V. Mendes et al [19] presented an analytical approach based on the double multiple stream tube model to estimate Darrieus turbine performance. A new design of Darrieus turbine design has been produced based on the presented approach results, a design which is supposed to be able to self-start and have an adequate performance at high tip speed ratios. Tests results were also provided as a validation of self-start, low noise, and stable performance of the proposed design.

J. Strickland et. al. [12] have formulated an aerodynamic prediction model for Darrieus turbines using a vortex lattice method. Experiments were conducted on a series of two-dimensional rotor configurations in a water towing tank. The agreement between predicted and experimental results was good. The presented model was suggested as an accurate prediction tool of instantaneous aerodynamic forces on turbine's blades and to characterize the near wake flow behind the rotor.

Blackwell BF, Sheldahl RE, and Feltz LV [13] have carried out a comprehensive experimentation for two and three bladed Darrieus wind turbines of a 2 meters diameter. Turbines have been tested in the LTV Aerospace Corporation Laboratories in the seventeens of the last century. Two different testing methods were employed: constant turbine rotational speed with variable tunnel speed and constant tunnel speed with

variable turbine rotational speed. Power coefficient as a function of tip-speed ratio for each configuration was presented. In that study, collected data, data reduction methods, and uncertainty analysis were discussed clearly, which made it an important resource for later research efforts.

A creative idea was introduced by P. Tchakoua and Co-workers [24]. They proposed a novel equivalent electrical model (EEM) for the Darrieus turbine. The idea is to be able to utilize analysis methods in the electrical engineering field by building a similarity model that transforms Darrieus turbine into an equivalent electrical circuit. The proposed model was built from the mechanical description given by the Paraschivoiu double-multiple stream tube model [27], based on the analogy between mechanical and electrical circuits. Physical concepts and theoretical formulations used for the model development were addressed in the article. Results were compared to corresponding analytical results obtained by DMST method with good matching for both normal and tangential forces on the blade.

While most numerical and experimental studies on Darrieus turbines discussed steady wind speed conditions, F. Scheurich and R. E. Brown [26] tried to discuss the effect of wind gusts on Darrieus turbine performance. In fact, steady wind conditions present an artificial environment for Darrieus turbine, as wind naturally experiences constant changes in speed and direction at the actual field. To address this issue, authors used a numerical method called vorticity transport model (VTM). Comprehensive results were reported regarding the blade's angle of attack, turbine's power coefficient and wake structure. The authors ended up with important conclusions implying that wind speed variations affect negatively on performance; power loss relative to performance in steady wind conditions was reported.

Computational Fluid Dynamics is thought to provide an essential contribution to the development of Darrieus turbines in the near future. CFD offers a lower cost advantage compared to laboratory experimentation. Also, much more details can be revealed using CFD including turbine operation and wake structure. On the other hand, proper

discretization and accurate modeling of the problem is needed to get useful results from simulation. F Balduzzi et. al. [15] have carried out an extended investigation on the published literature, with the aim of identifying the most effective simulation settings to ensure a reliable simulation procedure for straight blade Darrieus turbine. The main analysis parameters have been selected and their influence has been analyzed; like domain dimensions, turbulence model, and angular step increment. After that, the selected settings were applied to simulate the geometry of a real rotor which also has wind tunnel test's results. Finally, good agreement between numerical estimations and experimental data has been noticed. In addition, the proposed approach was further validated by comparing its results with two other sets of simulations from literature.

Darrieus turbine is thought to minimize the huge land resources required for wind turbines' farms. The limited availability of lands and utilizable wind resources implies heading to smaller footprint wind farms. Darrieus turbines can offer better performance with a smaller distance between adjacent rotors, working as an interactive pair of turbines [10]. Vergaerde and co-workers used experimental methods to study a pair of closely spaced turbines. They found out that the coefficient power can increase up to 16% [11]. In the same context, J. Hansen, M. Mahak and I. Tzanakis utilized 2D CFD methods to analyze the performance of both an isolated and pair of Darrieus turbines. An enhancement by 15 % in power output was reported for the pair configuration relative to the isolated turbine. On the other hand, the performance of paired Darrieus turbines appeared to depend significantly on wind direction unlike the isolated turbine case [17].

J. Bremseth and K. Duraisamy [25] has investigated single, pairs, and arrays of Darrieus turbines numerically, with an objective of understanding the underlying flow structures and their implications on energy production. They also discussed similarities between the pair of Darrieus Turbines and pairs of rotating cylinders, in terms of wake structure and vortex shedding. As a result, they found that the aerodynamic interference between turbines gives rise to regions of excess momentum between turbines, which can lead to significant power augmentations for downstream columns, such that it can be more

efficient than leading columns; an important result which could lead to great improvements in wind farm productivity.

Different research methodologies for studying Darrieus turbines were witnessed in literature. More focus on analytical approaches appears in earlier studies, while numerical simulation is dominating the more recent research stream. Analyzing the performance of an isolated turbine was the core of most research efforts, while a smaller number of studies have discussed the paired turbines. Within the part of studies which focused on matched turbines, the usual target was to inspect the possibility of energy production enhancement in case of paired or arrayed turbines, without a detailed understanding of the case. As mentioned by [17], many factors affect the matched turbines' operation like; wind direction, center to center distance, and the direction of rotation. This study aims to optimize distance between a pair of Darrieus turbines to enhance the pair performance, using numerical simulation methodology, validated with experimental results reported by Vergaerde et. al. [11].

# Chapter 3

## Methodology

### 3.1 Introduction

Flow field through Darrieus turbine is a complicated case due to mutual interaction between upwind and downwind machine's halves. Theoretically, wind's velocity goes through several stages as shown in figure 3.1. Starting from the free stream conditions far away before turbine, then reaching the induced velocity just before entering the turbine. While wind is passing through the upwind half, part of wind's energy is being harvested by blades in upwind region, which lowers the velocity to reach equilibrium velocity at midplane between rotor's halves. When flow approaches the downwind half blades, velocity is called downstream velocity. Finally, it exits the turbine at wake velocity.

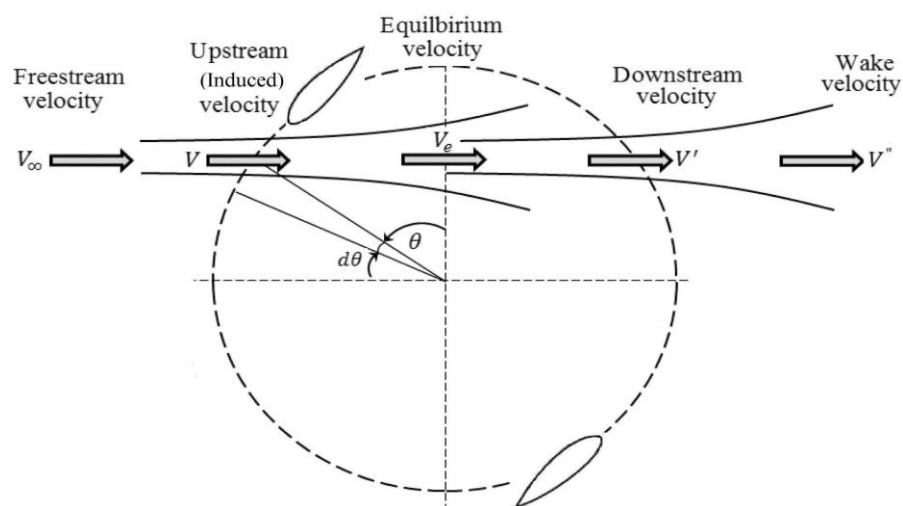


Figure 3.1: Velocity stages through Darrieus turbine

As Darrieus turbine rotating, blades experience a constant change in the angle of attack with fluid stream while they are rotating, as previously shown in the figure 1.10. This rapid oscillation in angle of attack produces in turn oscillating lift and drag forces which adds more challenges on performance prediction accuracy. Moreover, blades rotation in a circular path induces a curvature effect such that blades behave like a curved blade [14], which adds more complexity to Darrieus turbine analysis.

Darrieus turbine's blades rotate in such a way that keeps the flow around airfoil changing between the attached and separated flow modes, due to the rapid oscillation in the angle of attack, which induce more complexities in flow physics presented in dynamic stall effect. Dynamic stall imposes a different stall graph than static one, so that the blade's lift stalls earlier and more steeply, while the flow returns to attached mode later than the case of static or slow changes in angle of attack.

On the other hand, an inherent advantage of Darrieus turbine mechanism is the ability to utilize Katzmayr effect. This effect is noticed to occur in case of oscillating flow around airfoil, or in case normal flow around oscillating airfoil, as a thrust force component is noticed to be produced. Katzmayr effect may not generate a high amount of thrust, however it still has a significant increase in lift coefficient, noting that the shape of trailing edge is critical for this effect's magnitude level.

As discussed above, blades behave in Darrieus turbine differently from other common aerodynamics applications like aircrafts. Such that even if the incident flow's velocity is possible to be determined for all blade's azimuthal positions, still another question is how the blades will interact with the incident flow when taking into account curvature effects, dynamic stall, and Katzmayr effect. This combination of complex effects exist in Darrieus turbine flow field may also produce a mutual and secondary effects, which change how blades react to wind incidence from the normal behavior. Most of the available experimental observations and reported airfoils coefficients, are coming from common aerodynamics fields like aircraft studies, but Darrieus turbine analysis seems a unique case of study.

## 3.2 Darrieus Turbine Analysis Methods

As mentioned in the second chapter, mainly three kinds of methods are intended to estimate performance characteristics of Darrieus turbine: analytical, experimental, and numerical methods. While the analytical methods were preferred earlier, like in the seventies of the last century, numerical and experimental methods showed more ability for development attached -mainly- with computers development. Darrieus turbine experimentation keeps a preferred way to get actual insight about the machine operation as it shows the actual performance data; however, laboratory tests are carried out in ideal conditions which are not similar to site conditions at all, since site's wind is gusty and irregular. Also, experimentation is an expensive option to carry out experiments for the Darrieus turbine since it is attached with a need for complex apparatus.

### 3.2.1 Analytical Methods

The most common analytical method for Darrieus turbine analysis is the double multiple stream tube method (DMST), which was developed by I. Paraschivoiu [27] as an upgrade of a simpler method called stream tube method. Those methods were outweighed with modern numerical methods, as a more reliable option to get accurate results for Darrieus turbine performance estimation. However, understanding earlier methods can be important in order to implement numerical methods more efficiently, also analytical results can be used for the numerical results verification. Furthermore, it is recommended to start with simple analytical calculations as a preliminary design stage of Darrieus turbine before proceeding to numerical analysis.

Stream tube method assumes single velocity for fluid crossing the rotor, while multiple stream tube models allow for many values to increase the accuracy. All stream tube methods are based on dividing flow domain (swept area) into a series of adjacent aerodynamically independent parallel stream tubes, then, equating forces on the blade to streamwise momentum change through the rotor based on the blade element theory, and

finally get a solution with using available databases blades lift and drag coefficient. In turn, blade element theory based on momentum conservation and equilibrium assumptions, states that that torque exerted by rotors has to be equal to the momentum change. This theory is applicable only for lightly loaded rotors, operating at low or moderate relative TSR to get acceptable results. In addition, stream tube methods are limited to low solidity i.e., below 0.2, and for low chord to radius ratio below 0.1, since at high TSR, its momentum equations become invalid, and predicted blade loads are inaccurate as these models assume quasi-steady flow through the rotor.

### 3.2.2 Experimental Methods

The most direct method to test Darrieus turbine performance is laboratory test, as it reflects the actual behavior of the machine in real life. However, experimental testing suffers from difficulties like high cost, complexity, blockage, and noise effects. Another issue that testing in the laboratory is usually carried out at regular wind speed which is totally different from the gusty wind behavior on site, so it provides a limited look at the performance within ideal conditions. Open, semi open and closed wind tunnels apparatus can be implemented to test Darrieus turbine performance, but closed wind tunnels suffer from significant blockage effects induced by wall presence. Experimental apparatus usually includes a turbine model, wind source, measurements devices, and data management and reduction system. It is also important to check for systematic errors and define the uncertainty level for experimental testing.

### 3.2.3 CFD

The development of computers enhanced numerical methods (CFD) abilities as a practical option to handle Darrieus turbine analysis. Numerical simulation of any physical problem provides results sensitive to the procedure followed for approximating the real-life problem, into a set of equations and parameters and then solving it. Many previous studies tried to provide enhanced simulation methodologies [15, 17, 28], but



still there is no final answer regarding defining a clear analysis procedure. CFD owns the advantages of economical cost as in analytical methods. It is able also to consider all possible physical effects as experiments do, including dynamic stall, curvature and Katzmayr effects. Darrieus turbine analysis treats highly different scales in time and space domains as explained in table 3.1 below. Such wide variety of scales for each parameter adds a complexity to the analysis and requires more attention to validate numerical procedure and verify the results.

Table 3.1: Scales limits for main analysis parameters [29]

	length scale (m)	velocity scale (m s <sup>-1</sup> )	time scale (s)
aerofoil boundary layer	10 <sup>-3</sup>	100	10 <sup>-5</sup>
aerofoil chord	1	100	10 <sup>-2</sup>
rotor	100	10	10
cluster	1000	10	100
wind farm	10 000	10	1000

Predicting physical effects at small and large scales as mentioned above, simultaneously and adding them up to get the solution, may cause errors or miss-accuracy unless the procedure followed is structured well. More attention should be paid to certain physical quantities, at certain locations of the domain such as Reynold’s number and courrant’s number in order to assure results’ quality. Such parameters can be used to ensure that the physics of the problem keeps “likely” correct while simulation is going on.

CFD presents an attractive option due to its uncountable advantages, as it is an economic, easier way to analyze Darrieus turbine operation relative to other methods. Also, it has a great potential to provide accurate results even though it doesn't guarantee results accuracy, unless a dedicated results verification process is applied. Generally, CFD results need to be compared with results from experimental sources to assure the validity of results, and prove modelling methodology. After being sure about the methodology strength, it can be used to analyze new cases - carefully.

CFD analysis presents a promising solution to enhance the design process and reliability of the Darrieus turbine. It provides the ability to investigate, calculate and plot all flow parameters efficiently with comprehensive details regarding expecting power production, structural reliability, and lifetime of the Darrieus turbine. Many studies have shown good ability for CFD to solve the flow field through Darrieus turbine verified with experimental results [15,21,23].

Validation and verification are important steps in the CFD simulation procedure. Validation is the process of determining whether the numerical model -conceptually- is an accurate representation of the actual system being analyzed. So, it assures that the concept is translated to the correct system of equations. Verification is the process of determining if numerical code is working properly, and providing results consistent with the corresponding results from experimental, analytical or numerical sources. Also, numerical verification techniques can be used, like mesh independency test and results convergence check, which will be applied within this study as explained further in the following parts.

### 3.2.3.1 Numerical Modeling

Radial symmetry in rotary machines usually facilitates modeling with simpler model and lower computational requirements; however, the absence of any symmetry in the case of Darrieus turbine, implies a transient analysis for the whole domain. CFD analysis starts with creating a geometrical model, then setting up a numerical model approaching the physics of the real problem as possible. The first step for CFD analysis is to select or write a CFD code, in our case here, we selected ANSYS FLUENT due to its good reputation, resources availability, and strong attendance in literature. In addition, Fluent comes within ANSYS workbench software package, that provides a state of art environment including tools to manage geometry creation, meshing, setup, solution, and post processing stages. After having the CFD code identified, the next step is to create a suitable domain in shape and dimensions as well as define geometry and objects included. Following the geometrical domain becomes ready, it is discretized to a grid of

elements with small sizes and intense distribution, enough to capture the important flow features (meshing). Setting boundary conditions is the next step, where we define physical conditions for each part of domain, similar as possible to the real-life problem. Before starting the solver, all settings are adjusted in an order to solve the problem efficiently. Finally, after getting the solution it can be processed into a certain set of useful outputs.

Straight blades Darrieus turbine's numerical modeling has three options regarding the analysis dimensions: 2D modeling, 2.5D modeling, and 3D modeling. 2D modeling is the most common and easier option, as it is done in a planar domain which implies simpler model, attached with lower computational power needs. However, 2D modelling is not the best option for results accuracy, as it suffers generally from a tendency to results overestimation referred to neglecting factors listed below:

1. Tip losses
2. Span wise gradients
3. 3D turbulence structures
4. Parasitic losses (struts losses)

On the other hand, 3D analysis option requires a huge computational power, which makes it not a practical choice in most cases, especially at the preliminary design stage. Most relevant studies present 2D simulations instead of 3D with trying to enhance modeling procedures to get more accurate results. Another option is to implement 2.5D modeling choice, which means to simulate partition of the axial span of rotor's geometry, with periodic conditions applied at the ends in the axial direction. This method is assumed to be useful to account -partially- for span wise effects, also to have a closer model to the real case as the problem nature is three dimensional.

### 3.2.3.2 Mathematical Background

- Navier-Stokes Equations

The Navier-Stokes equations shown below, are differential equations that can be used to mathematically model the behavior of any Newtonian fluid in any flow regime [30]

$$\frac{\partial \rho}{\partial t} + \nabla \cdot (\rho \mathbf{u}) = 0 \quad 3.1$$

$$\frac{\partial u}{\partial t} + \mathbf{u} \cdot \nabla \mathbf{u} = -\frac{1}{\rho} \nabla p + \eta \Delta \mathbf{u} + \mathbf{g} \quad 3.2$$

Equation 3.1 is mass conservation equation, and equation 3.2 is momentum conservation equation, it can be also reformed into three equations in x, y, and z directions. Navier-Stokes equations have no analytical solution yet, so numerical methods are implemented to solve it. Even solving those equations directly is possible using numerical methods, but still, it requires a huge computational power, making direct solution not a practical option. To simplify those set of equations, Reynolds averaging method is implemented which produces a modified set of equations called RANS equations.

- RANS Equations

RANS stands for “Reynolds Averaged Navier-Stokes”. The idea here is to decompose quantities in N-S equations from instantaneous (exact) form into two components; time-averaged and fluctuating components as shown in equation 3.3:

$$\phi = \bar{\phi} + \phi' \quad 3.3$$

Applying this approximation turns out a new set of equations called RANS equations as shown below;

$$\frac{\partial \rho}{\partial t} + \frac{\partial (\rho \bar{u}_i)}{\partial x_i} = 0 \quad 3.4$$

$$\begin{aligned}
& \frac{\partial}{\partial t} (\overline{\rho u_i}) + \frac{\partial}{\partial x_j} (\overline{\rho u_i u_j}) = \\
& -\frac{\partial(\overline{p})}{\partial x_i} + \frac{\partial}{\partial x_j} \left[ \overline{\rho} \left( \frac{\partial u_i}{\partial x_j} + \frac{\partial u_j}{\partial x_i} - \frac{2}{3} \overline{u_{ij}} \frac{\partial \overline{u_m}}{\partial x_m} \right) \right] + \frac{\partial}{\partial x_j} (\overline{-\rho u_i' u_j'}) \quad 3.5
\end{aligned}$$

Regarding the fluctuating terms  $\overline{u_i' u_j'}$  which appear in RANS equations, it is not possible to be calculated directly. So, another approximation process is needed to approximate them, which is called “turbulence modelling”. The aim of all turbulence models is to approximate the fluctuating components terms using theoretical assumptions and empirical relations. Boussinesq has related Reynolds stresses term  $\overline{u_i' u_j'}$  to velocity gradient through artificial proportionality constant, called eddy viscosity  $\mu_t$ . Many common models were formulated based on eddy viscosity concept, like k-w and k-s models. The main difference between all eddy viscosity models is how to calculate the eddy viscosity itself.

### 3.2.3.3 Turbulence Model Selection

Turbulence modeling is an averaging process for fluctuating flow quantities, using semi empirical formulations. The better turbulence modeling is the one that has the lowest complexity, while captures the essence of the relevant physics within moderate computational requirements. Selecting the most suitable turbulence model is critically important for analysis’ outputs accuracy. Commonly, k-w and k-s models are implemented for Drrieus turbine simulation through relevant literature. Both models were recommended for use, k-w model has good abilities to calculate near wall region besides wake and separation zone, but it misses some accuracy in free stream region. Vice versa k-s model is not able to predict separation zones and near wall region accurately, while it works well in free stream. Both models have problems of over predicting wall shear stress. To overcome shortages of standard k-w and k-s models, a modified k-w model was introduced by Menter [31] called Shear-Stress Transport Model (SST). The SST k-w turbulence model is supposed to demonstrate better accuracy among other RANS turbulence models, but when used with sufficiently refined spatial and temporal discretization.

### 3.2.3.4 Meshing

Meshing procedure and grid's quality are a critical input which determine significantly the overall accuracy of the CFD analysis' results. Due to the complex flow behavior in Darrieus turbine, meshing step requires attention to ensure capturing necessary flow field details. Using unstructured mesh in rotating regions is preferred, as it mitigates the sensitivity of the grid to flow's directionality, on the other hand, structured mesh offers a lower computational load. Smooth transition should be ensured for both structured, and unstructured mesh through different domain parts. Smooth transition aims to have a relatively similar volumes for cells in adjacent, in order to avoid any creation of artificial gradients which can be induced if sudden transitions exist [32]. Mesh resolution should be set based on the expected gradients intensity, in order to accurately compute the spatial variation of flow quantities and limit the numerical diffusion.

Certain grid quality-measures can help in better mesh creation, like Y-plus ( $Y^+$ ) and courant number.  $Y^+$  is a dimensionless distance indicator, helps to determine the location of the near wall elements relative to the boundary layer thickness. Capturing near-wall flow details owns a critical importance to calculate the rest of the flow field correctly. Fine prism layers are usually introduced next to blade's wall, figure 3.2. High gradients existence in near-wall region implies smaller elements enough to ensure calculation accuracy, while  $Y^+$  acts as a tool to decide the suitable size of layers next to blade.

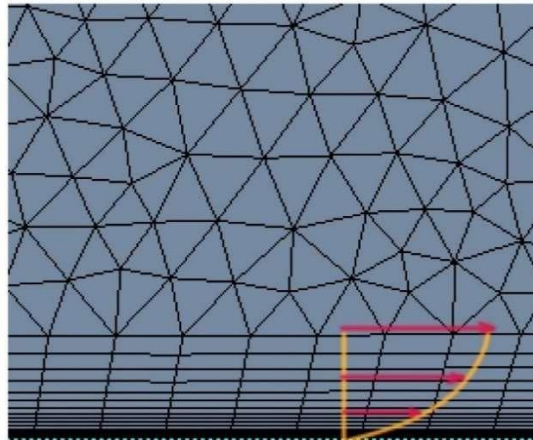


Figure 3.2: Prism layers

The distance between wall and the adjacent layer element's center is calculated by  $Y^+$ . R. Lanzafame et. al. [33] advised to keep  $Y^+$  below "1" to calculate the first layer thickness based on the equation 3.6 below.

$$Y^+ = \frac{y \rho_c}{\mu} \quad 3.6$$

Such that  $\rho_c$  is called friction velocity,  $y$  is the distance from the wall to the center of the first layer, and  $\nu$  is the kinematic viscosity of the fluid. An additional advice by S. Zanforlin and T. Nishino [34] is to have the first layer thickness of "2.3E-4" of the chord, while F. Balduzzi et. al. [35] advised to have the total prism layers thickness within the order of 3% of the chord. In addition, the distribution of elements around blade plays an important role in outputs accuracy. Both leading and trailing edges of the blades should have finer elements distribution, since flow characteristics at leading and trailing blade's edges controls significantly the flow nature around the rest of the blade. Also, the element size in chord-wise direction is advised to be within 0.002 of the chord length as followed by [34].

To allow blades rotation, a part of the geometrical domain should be defined as a rotating region, which will be a circular region with a center coincides with rotor's center. Elements within this rotating region should be finer than the rest of domain as it presents the core which contains the most important flow field's events. At the border between rotating and static regions, a non-conformal sliding mesh interface should be defined to ensures flow field connectivity while elements moving at the inner side. Non-conformal interface means that boundaries between cell zones allow mesh node locations to be not identical, but it permits the boundaries to exchange fluxes. Element size at interface should be within "0.1" of the chord length or smaller, according to F. Balduzzi et. al. [35].

### 3.2.3.5 Boundary Conditions

In CFD analysis, boundary conditions' definition aims to control the interaction between flow field elements in order to approach real-life physics modelling, closer as possible. Starting from external domain boundaries down to the blade's wall, each element should have a condition characterizes how it acts; like wall, inlet, outlet, etc. Later in this chapter, an explanation for boundary conditions implemented in our study will be presented.

### 3.2.3.6 Solver Settings

After the problem is modelled numerically, CFD code is used to provide a numerical solution for the set of equations and conditions prepared in modeling steps, over the created grid in meshing step. Most of commercially available codes are general purpose codes, which allow user to customize solver's parameters to be more suitable and stable while processing the case's inputs. Firstly, solution scheme should be selected, each solver provides several options, in Fluent case, "Simple", "PISO", and "Coupled" schemes are the main candidates. "Simple" schemes may provide good accuracy with low computational requirements, however, "Coupled" scheme ensures better accuracy for complex cases, also it has less sensitivity to time step.

First order and second order solution discretization options are offered in Fluent. At the beginning of simulation, first order can be used to stabilize the solution, then it should be switched to second order to ensure more accuracy. Another important option to set, is the residuals, which represent the allowed deviation of the numerical solution provided by subsequent iterations with relative to each other. Lower residuals imply more accurate solution, but increases the time required to solve the problem. Residuals in Fluent are scaled quantities, dimensionless have no units. Generally, residuals down to "1.0E-4" should be enough for the case under study [34].



### 3.2.3.7 Time Step

Angular marching step size has a great effect on overall results accuracy. A lot of errors can be produced if the angular marching step is too coarse. Generally, increasing time step increases nonlinearity effects, which introduces a local oscillation to the solution causing unsteadiness. On the other hand, using finer time step instead of certain limits may introduce also unsteadiness.

### 3.2.3.8 Results Reporting

One of the great advantages of CFD its ability to have a full sort of results for any physical quantity needed, in a clear graphical and/or numerical form. Within this study, the following parameters will be reported. Moment production is provided to compare results from different mesh grids and to check solution convergence between subsequent operation cycles. Power factor is reported with aim to express the efficiency of the turbine under study, as well as compare it with corresponding results from experimental sources. Courant number will be discussed later in this chapter, as it presents an important parameter for CFD transient analysis, since it relates between spatial and temporal discretization.

## 3.3 Current Model

In this study, a double-bladed straight blades Darrieus turbine analysis, both for single turbine and a pair of turbines cases will be discussed. In this section, single turbine simulation methodology will be presented, with verification by experimentally produced results for a same turbine design at similar operational conditions. Firstly, turbine geometry and surrounding domain will be defined. Then, suitable discretization for space domain is applied, and then turbulence model is selected. After that, boundary conditions are set similar to the actual case parameters. Solution scheme and solver parameters are then calibrated. Finally, outputs are prepared for verification.

In order to carry out results verification, we considered comparing our numerical results to experimental results. A. Vergaerde et. al. [11] have presented an experimental result for a double-bladed vertical axis wind turbine shown in figure 3.3. Full description of the turbine is provided in their study, including geometrical model and operation conditions details which are required to carry out the numerical analysis. Table 3.2 below shows main parameters that describe the experimental apparatus.



Figure 3.3: Experimental apparatus used by [11]

Table 3.2: Main experimental parameters

Experiment type	Wind tunnel
Free stream velocity [m/s]	11
TSR range [-]	2.5 ~ 3.25
Turbine construction	2 bladed straight blade type
Blade airfoil profile	NACA 0018
Chord length [m]	0.05
Rotor diameter [m]	0.5

Blockage correction applied	No
-----------------------------	----

A set of CFD simulations were conducted within this study at different TSRs and for different grids, in order to have a proved methodology as possible and verify results. The problem has modelled into a 2D problem using a horizontal section of rotor's geometry. 2D modeling is more common in literature than the 3D one, as it can achieve relatively good results as discussed in chapter 2. Furthermore, it helps to get results faster even with limited computational resources. In this section, our simulation procedure will be discussed. Clarifying details and steps followed to get the results presented in the following chapter.

### 3.3.1 Geometry

Double bladed straight blades Darrieus turbine is discussed here, featured with NACA 0018 profile for blades, with whole rotor diameter 0.5 m, and chord 0.05 m. Rotor's solidity is 0.2 according to the equation 1.2. Inclined NACA 0024 shaped struts were used to connect blades to the rotating shaft. Figure 3.3 below depicts the geometry of the turbine under study. In our 2D simulation, only blades were modelled, as it's not applicable to model struts into 2D, while its optional to include shaft's cross section.

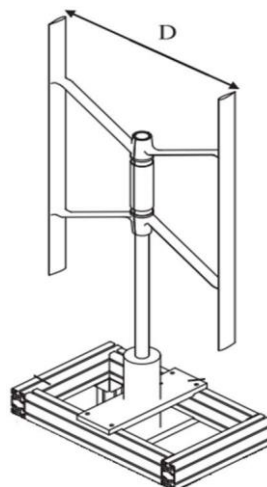


Figure 3.4: Actual Turbine's geometry

### 3.3.2 Geometrical Model

Numerical domain is created with three main members: blades, rotor region, and surrounding field region, see figure 3.5 below. A circular region containing the blades is created with diameter slightly larger than rotor's diameter, will act as a rotating region. Elements in this region rotates as rigid bodies, at speed same as rotor's speed, retaining same shapes and volumes of all grid elements. Modeling in this way is more stable than dynamic mesh option, which rotates blades not the surrounding region, since the latter allows for cells deformation. Sliding mesh interface was set at the border between the rotating region and the rest of the domain. Regarding external domain dimensions, F Balduzzi et. al. [15] mentioned that it is important set of far-field domain boundaries far away, until the solution becomes independent of domain size changes. Domain sizes are summarized in table 3.3 based on recommendations by F Balduzzi et. al. [15], they decided that larger domains did not affect the solution further in terms of torque prediction.

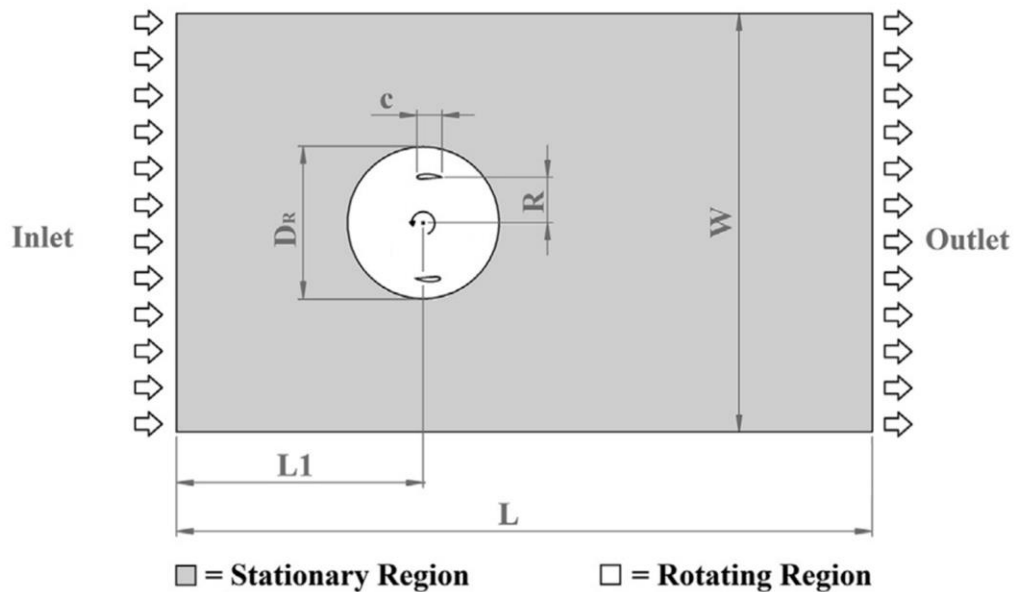


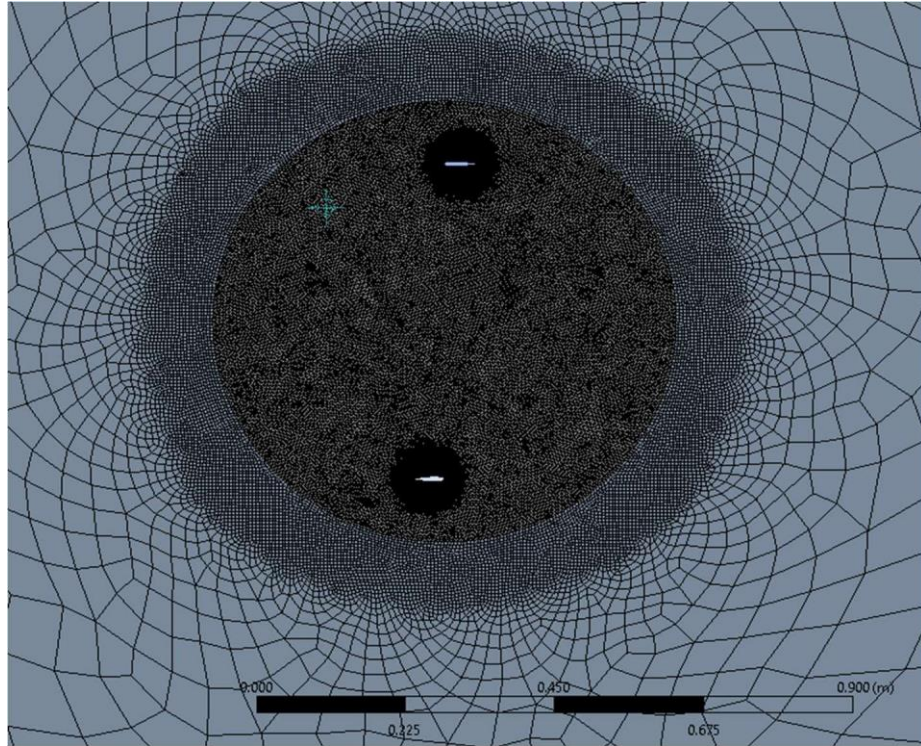
Figure 3.5: Computational Domain

Table 3.3: Domain dimensions relative to rotor diameter

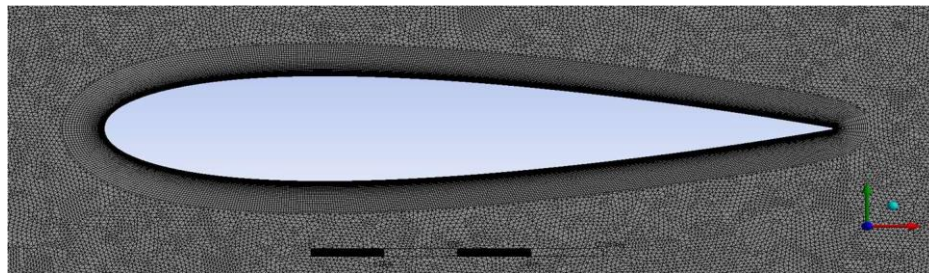
Quantity	Value
Total Domain Length (L)	90 D
Distance from Inlet to turbine (L1)	30 D
Domain width (W)	60 D
Rotation region diameter $\square_R$ (single turbine model)	1.4 D
Rotation region diameter $\square_R$ (pair of turbine model)	1.28 D

### 3.3.3 Meshing

Meshing step critically affects CFD results accuracy. Relatively, a very fine mesh is necessary to capture gradients and flow features well, especially for a complex flow field like this case under discussion here. Domain is discretized using an unstructured mix of Tetra and Hexa elements' types, except in the airfoils' near-surrounding region, where a structured prism layers are created in order to resolve boundary layer regions with proper accuracy. Figure 3.6 below illustrates the grid structure used to discretize the domain; part (a) of the figure shows mesh structure for the whole rotor, while part (b) depicts mesh structure around a blade.



(a) Mesh structure for rotor's region



(b) Mesh structure around blade

Figure 3.6: Mesh structure

In order to study solution-grid independency, creating multiple grids is common practice to test solution sensitivity to grid refinement. Five mesh grids were created taking into account related literature's recommendations, grids are started with relatively coarse elements sizes for grid 1, and then refined gradually reaching the finest for grid 5. The total number of elements ranged between 58k to 680k as clarified in table 3.4 below.

Table 3.4: Grids details

Grid	Total number of elements	Thickness of first prism layer [m]	Number of prism layers	Number of nodes at airfoil wall	element size at airfoil's control circle [m]	element size at interface [m]
1	58276	5.0E-05	30	250	8.0E-04	0.02
2	120571	1.0E-05	35	350	5.0E-04	0.02
3	172198	1.0E-05	35	400	4.0E-04	0.015
4	292985	2.0E-06	50	600	3.5.0E-04	0.006
5	678873	1.0E-06	70	900	2.5.0E-04	0.003

Moving from grid 1 to grid 5, grids are refined gradually with keeping almost the same structure, but with finer elements everywhere through the domain. Main features of all grids are listed below:

- 1- Inflation layers
- 2- Refinement circle around blade
- 3- Refinement circle for rotating region including interface region
- 4- Gradual transition

Those features were included in order to increase calculation accuracy at certain regions and help to use the available computational power effectively.

### 3.3.4 Boundary Conditions

Boundary conditions are determined with the aim to approach the real case as possible. In the numerical domain which shown in figure 3.5 above; left-hand boundary of the domain is set to velocity inlet with 11 m/s magnitude, the right-hand boundary of the domain is assigned as pressure outlet, while the lateral sides are set to symmetry condition. Setting lateral walls to symmetry condition means that stream wise velocity components are allowed parallel to wall components, which reduces the possible influences of the domain dimensions on the flow-field. Blades are given a non-slip wall condition. A mesh motion condition is assigned for the rotating region with rotation

speed differs according to TSR in each analysis case. The circular border of the rotating region is assigned as a sliding-nonconformal mesh interface.

### 3.3.5 Turbulence Modeling

K- $\omega$  SST model is selected for turbulence modelling due to its advantages as mentioned in relevant literature [31]. It is assumed to treat near walls regions more accurately while keeping proper accuracy in free stream and wake regions.

### 3.3.6 Solver's Settings and Solution Strategy

Solver initiating should go gradually from easier to harder conditions until reaching full transient analysis mode, based on an advice by [15]. To enhance results accuracy and solver stability, a gradual path of numerical settings adjustment is followed. Solver's settings are started by running a steady state case with first order discretization scheme implemented, with no rotation motion applied. After getting the solution converged, analysis mode is switched to transient mode with keeping first order discretization scheme active. In the next step rotation is applied and solution is run to progress for 3 turbine's revolutions. Finally, the discretization scheme is switched to second order in time and space and the solver is started until solution become converged.

### 3.3.6 Time Step Selection

Based on CFL time step criterion advised by [36], time step can be calculated for the current case for grid 5:

$$\Delta t_{@interface} = \frac{u \Delta t}{\Delta x} = \frac{11 * \Delta t}{0.002} < 1 \quad \Delta t, \Delta x < 1.8 * 10^{-4} \quad 3.7$$

Based on the result above, time step should be below  $1.8 * 10^{-4}$  to comply with CFL criterion; however, we selected a time step of  $4 * 10^{-5}$ , to ensure a safer angular



marching and avoid any discontinuities. This selected time step is equivalent to 0.3 deg angular step at TSR of 3.

### 3.4 Solution-Grid Independency Check

A primary step while conducting CFD simulation is to check solution sensitivity to grid refinement, which ensures that the grid is well-structured and fine enough, especially at the critical regions where flow features should be captured precisely. Grid independency check helps to test solution's reliability by comparing results from different grids to each other. Number of elements should be increased gradually until solution become stable, although if the grid is refined further. The aim of this check is to ensure that more refinement will not affect the solution at least significantly. In this study, we provide a dedicated mesh independency test results for five mesh grids listed in table 3.4, all grids were tested one by one at multiple TSRs.

Analysis outputs for this part of study were moment production and power factor. Moment data is provided directly from Fluent in unit of [N.m], while power coefficient is a unitless quantity calculated using the average of moment and some other operational parameters. A brief explanation of power factor and its derivation is provided below with related mathematical formulas.

#### 3.4.1 Power Coefficient

For any energy conversion device, the main performance assessment criterion is the conversion efficiency assessment, which is represented by the power coefficient ( $C_p$ ) for Darrieus turbine case. Power coefficient measures the extracted power by turbine to the gross amount of power available in wind flow, equation 3.8 below shows a mathematical statement for  $C_p$ .

$$C_p = \frac{\text{Extracted power}}{\text{Available Power}} = \frac{P_{\text{turbine}}}{\frac{1}{2} \rho A_{\text{swept}} V_{\infty}^3} \quad 3.8$$

Such that  $P_{turbine}$  is the extracted power by turbine,  $\rho$  is fluid's density,  $A_{swept}$  is turbine's swept area, and  $V_{\infty}$  is the free stream velocity. For the case of 2D simulation, equation 3.8 above can be simplified to:

$$C_p = \frac{P_{turbine}}{\frac{1}{2} \rho A_{swept} V_{\infty}^3} = \frac{T_{avg} * w}{\rho * R * V_{\infty}^3} = \frac{T_{avg} * TSR}{\rho * R^2 * V_{\infty}^2} \quad 3.9$$

Such that  $T_{avg}$  is average torque produced by turbine,  $TSR$  tip speed ratio, and  $R$  is rotor radius. Commonly,  $C_p$  is plotted against  $TSR$  to produce a performance curve that shows turbine's efficiency variations at different rotation speeds. Figure 3.7 below shows a typical  $C_p$ - $TSR$  plot.

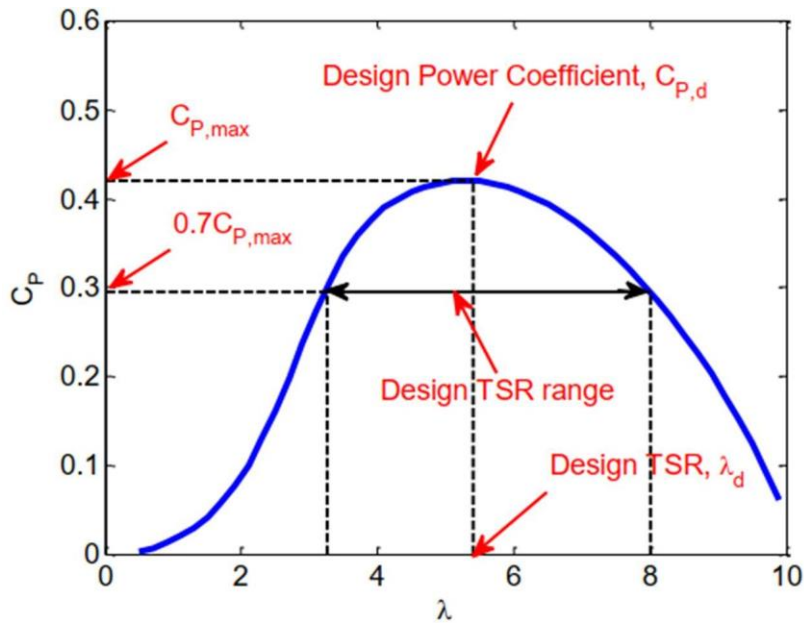


Figure 3.7: Typical  $C_p$  vs  $TSR$  [37]

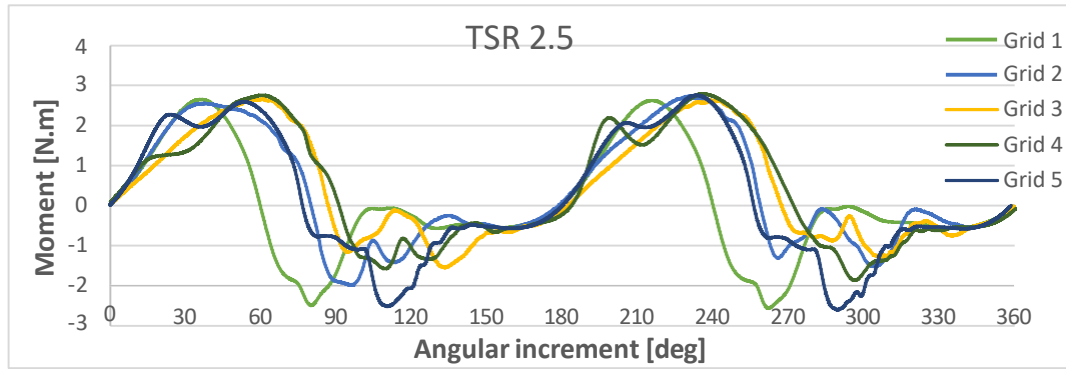
As shown in figure 3.7 above, Darrieus turbine shows a bell-shaped efficiency curve that has an optimum region almost at the middle, while the efficiency at both right- and left-hand side deteriorates as we move far from the optimum point. The left-hand side of the curve is the low  $TSRs$  region, where the operation faces instabilities while starting-up. The angle of attack at blades oscillates with higher amplitude at start-up which magnifies the effect of dynamic stall, lowers  $C_p$ , and increases flow field complexity.

After exceeding a certain TSR which depends on the rotor's design, the operation becomes in the optimum region, where  $C_p$  is relatively high, and keeps increasing with increasing TSR up to a certain value at which  $C_p$  starts to decrease if TSR increased. The region where  $C_p$  is higher than "0.7" of maximum  $C_p$  is called the optimum region of operation. The turbine should be designed to work within this region. Increasing TSR further after the maximum  $C_p$  is reached lowers the efficiency due to the effect of induced solidity. The rotor starts to act like a rotating cylinder preventing wind flow from passing through the blades, and so lower the energy available for harvesting within the turbines.

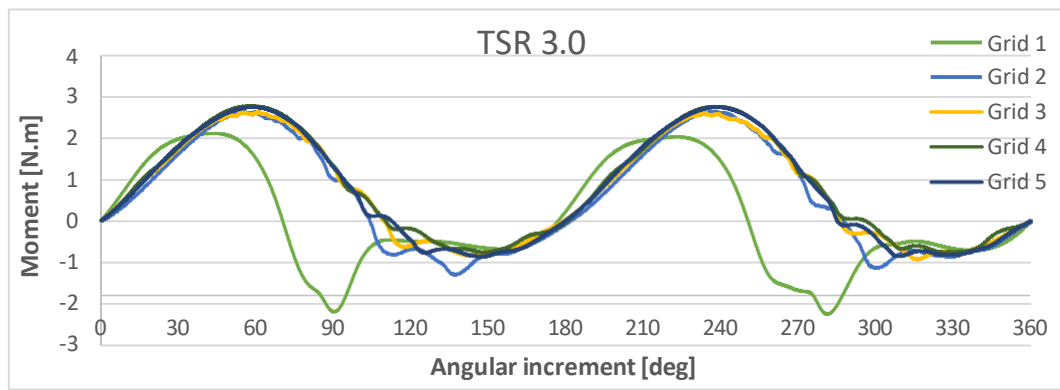
### 3.4.2 Solution-Grid Independency Results

To check if the solution can be independent from grid's refinement;  $C_p$  and moment data were reported for grids 1 to 5, at three TSR values: 2.5, 3.0, and 3.25 corresponding to the experimental data provided in a study by A. Vergaerde et. al. [11]. Experimental data from the mentioned study was selected as a basis for comparison, since it presents a recent experimental study based on reliable methodology, with accurate description provided for experimental apparatus and procedure in details. Moreover, it was important that the tested turbine implements a common airfoil profile NACA 0018, which was studied for decades in the scope of Darrieus turbine. Studying a common geometry is more helpful as it a participation in the main research stream, also it offers more resources for reference. According to results provided in [11], the turbine showed an optimum performance peak at TSR of 3.0, so the selected TSR values represent all different modes of operation; before and after peak region, as well the peak point itself will be studied too.

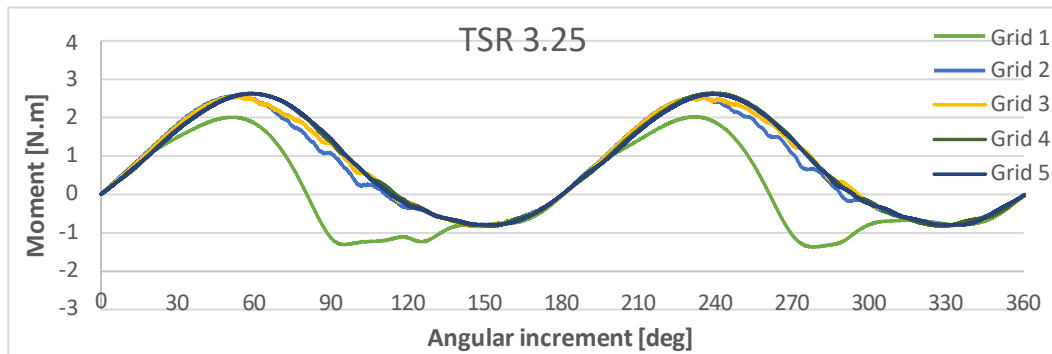
Firstly, we are going to show moment chart for a complete revolution of the turbine against the azimuthal angle, for all of the grids described above. The aim of presenting moment production for different grids is to notice grid refinement's effect on the solution behavior at different TSR values as shown in figure 3.8.



(a) Moment curve at TSR 2.5



(b) Moment curve at TSR 3.0



(b) Moment curve at TSR 3.25

Figure 3.8: Moment production plot for all grids at different TSRs

As shown in figure 3.8 above, curves produced at different grids showed a good matching at TSRs 3.0 and 3.25 for all grids except grid one. However, at TSR 2.5, curves didn't match well even with further grid refinement. Increasing the number of

elements is expected to affect the solution to a certain limit, then the solution should be stable however the number of elements is increased. This expected behavior can be seen for TSR 3.0, and TSR 3.25 clearly as the matching between grid 4 and grid 5 is almost exact. However, for the startup region i.e. TSR of 2.5, the behavior was different as the third and fourth grids showed some matching, but grid 5 showed a deviation from grid 4, certainly in spans between 90 to 120, and 270 to 300 azimuthal angle.

Figure 3.9 below shows power coefficient results for all grids at different TSRs. It is witnessed from the figure below that, increasing the number of elements further after the third grid didn't change  $C_p$  for TSR 3.25. On the other hand, for TSR of 3.0,  $C_p$  has increased slightly moving from grid 3 to grid 4, and then dropped down slightly for grid 5 to have almost the same value for grids 3 and 5. In similar manner, at TSR of 2.5,  $C_p$  kept relatively stable from grid 2 to grid 4, but it showed significant decrease with further refinement reaching grid 5.

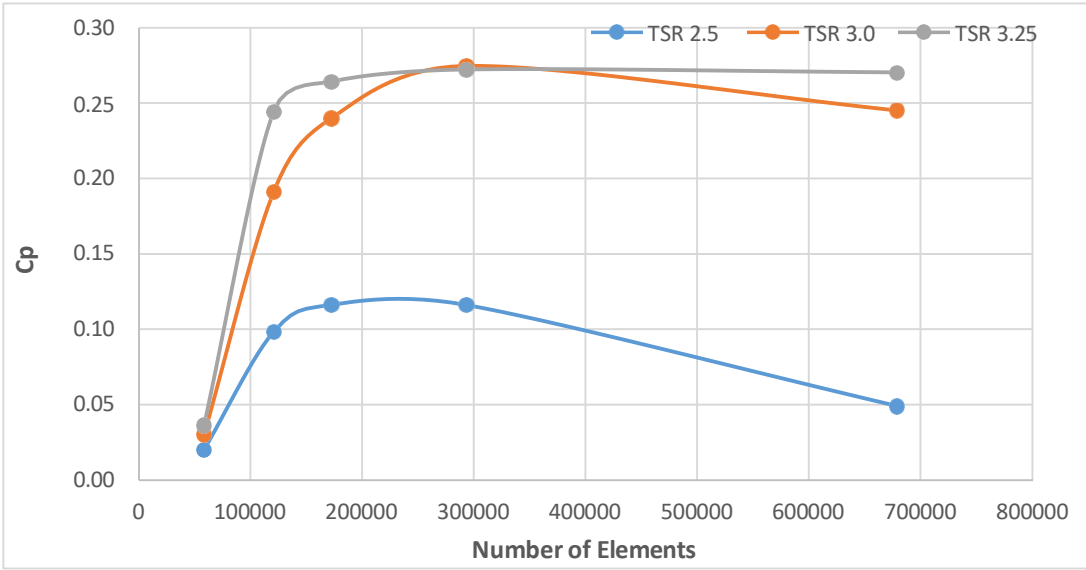


Figure 3.9:  $C_p$  versus number of elements at different TSRs

### 3.5 Convergence Criteria

Solution convergence in numerical simulation means to reach a stable solution independent from more iteration processes, like further iterations do not affect the solution significantly. This is ensured numerically by comparing residuals after each iteration to the targeted residuals values. Even reaching down to the assigned residuals itself has no actual physical meaning, and does not ensure solution correctness, but it is a step required within the numerical solution procedure. On the other hand, lowering residuals increases analysis' time since more iterations will be introduced, which implies that residuals can be lowered to a certain limit, trying to optimize both solution convergence and time requirements. S. Zanforlin and T. Nishino [34] recommended to set all residuals to  $1.0E-4$ . However, in our study, we set more strict residuals of  $2.0E-5$  for all residuals to ensure better accuracy.

In transient analysis of rotary machines, another convergence criterion should be applied by comparing results of subsequent rotations of the machine to each other. Convergence of the solution here is considered based on reaching a stable solution, complying with a certain allowable deviation of results for of further rotation introduced. Complying with this criterion ensures that the number of revolutions processed is enough to reach a stable solution i.e. within a 3% variation tolerance. K. M. Almohammadi [2] has mentioned that 10 rotations were enough for satisfactory results. In like manner, we found that our results agree with that recommendation as shown in figure 3.10 below.

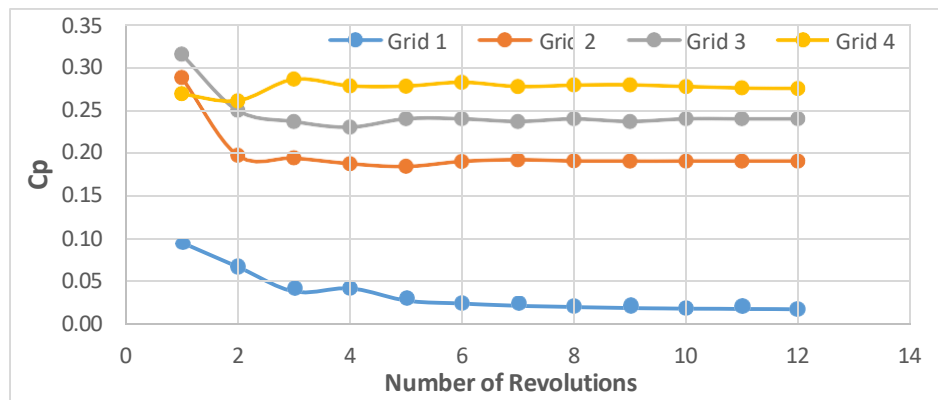


Figure 3.10: Cp variations through rotation progress at TSR 3.0

In figure 3.10 above, results showed a deviation below 1% for  $C_p$ , between two subsequent rotations after the tenth cycle. Also, instantaneous moment curve indicated almost an exact matching between subsequent cycles after the tenth one as shown in figure 3.11.

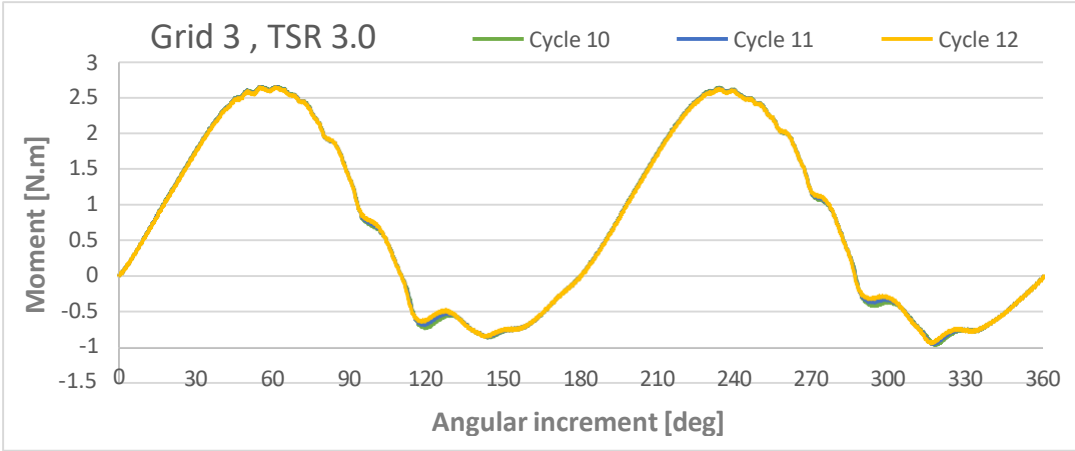


Figure 3.11: Moment curve for subsequent cycles

### 3.6 Courant Number Analysis

An important parameter in a CFD transient analysis is called Courant number. This parameter connects the temporal and space domains of the problem, it describes flow properties' advection through space in each time step relative to local grid size. Equation 3.11 below shows mathematical definition for Courant number.

$$C = \frac{v \cdot \Delta t}{\Delta x} \tag{3.11}$$

$v$  is flow velocity,  $\Delta t$  is time step, and  $\Delta x$  is distance between two cells centroids. Based on the equation 3.11, Courant number is ratio of solution propagation distance to the element size within a single time step, in other words, how many cells the flow crosses each time step.

Generally, in numerical methods, two solution schemes are used: explicit and implicit schemes. Explicit solution scheme requires the solution propagated within a single cell border in each time step, which implies a Courant number less than “0.7”. On the other hand, in implicit solution scheme solution’s propagation is allowed to exceed one or multiple cells border each time step, so courant number can exceed “1”, resulted accuracy depends on the nature of the problem. Figure 3.12 below explain both cases.

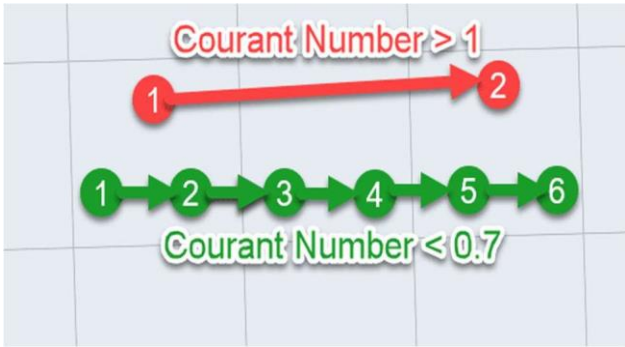
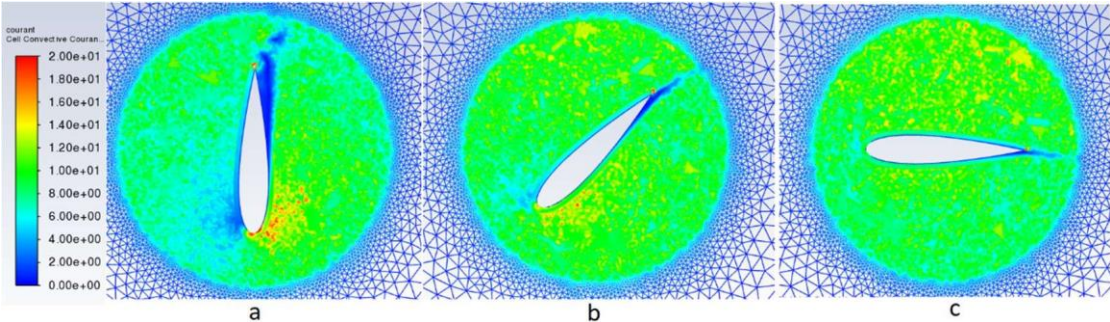


Figure 3.12: Clarification of courant number

Lower Courant number offers better accuracy as a general rule, since it limits instabilities amplification through domain and so, lower the chance for solution divergence. In our analysis, implicit solution scheme is implemented. However, due to flow field complexity in Darrieus turbine, a general agreement in literature advices to keep CO number below “10”. To assure our solution compatibility with low Courant number requirements, captures of courant number distribution around airfoils are presented in figure 3-13 for grid 3, and grid 5 at TSR of 3.0.





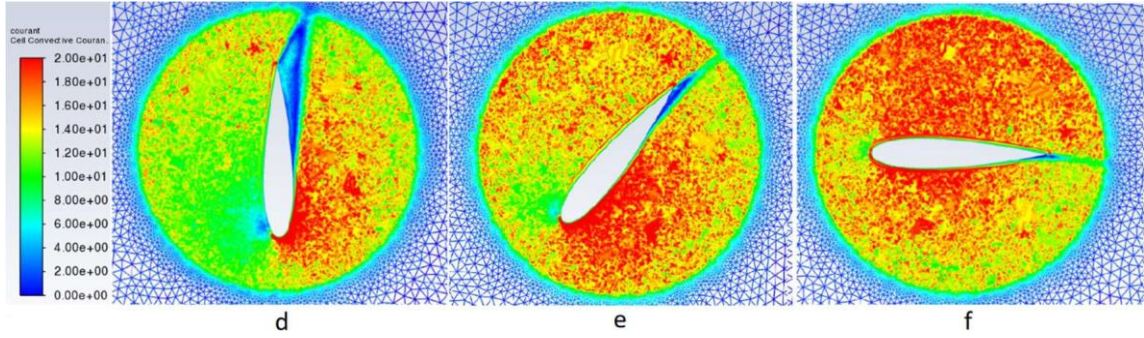


Figure 3.13: Courant number distribution for different azimuthal locations for grid 3 (a, b, & c), and grid 5 (d, e, & f)

### 3.7 Comparison with Experiment

In this section, our explained methodology's validity will be checked by comparing numerical results produced from 2D simulation, to results from selected reference from literature [11]. Figure 3.14 below shows our numerical results with its corresponding experimental data.

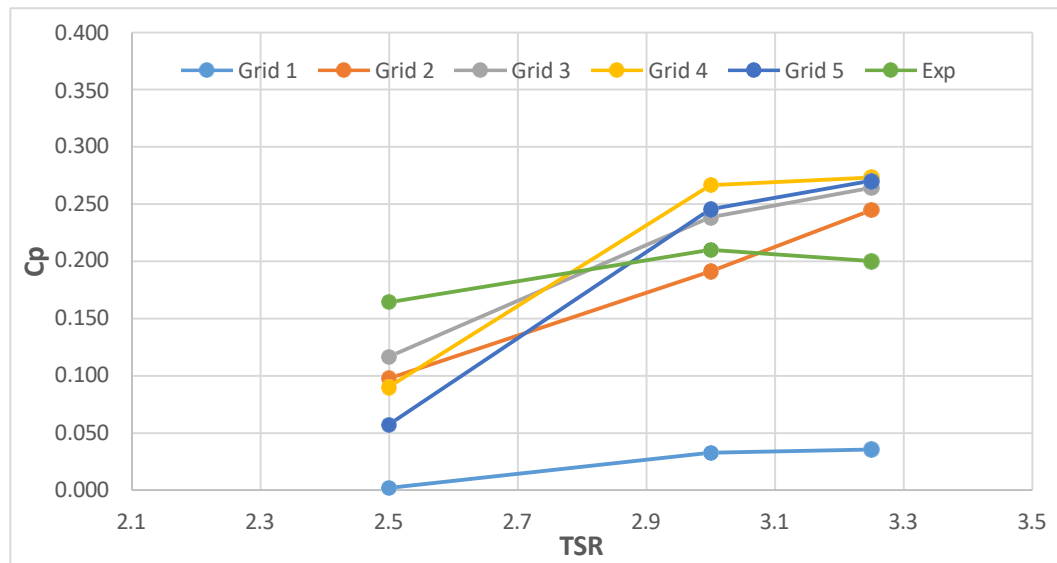


Figure 3.14: Comparison between Numerical and Experimental results from [11]

Excluding grid one, all grids have shown an acceptable matching with experimental results, although none of them has showed exact match. At TSR of 2.5 represents the

unstable (start-up) operation point within the range included, grid 3 was the closer to estimate  $C_p$  as experiment did, while further grid refinement reaching to grids 4 and 5 didn't improve the results or even keep it stable. Such behavior for finer grids can be referred to Courant number discussion, since finer grid produces higher  $Co$  at constant time step, which in turn may results in a deviation in results. At TSR of 3.0, both grids 3 and 5 have shown in between matching and closer estimation to the experimental  $C_p$ . Overestimation of about 15% is attendant but it can be acceptable due to 2D modelling approximation. At TSR of "3.25", grids 3, 4 and 5 have matched with each other, with overestimation of the experimental results reaching about 30%.

Our numerical results are compared to experimental in order to assure that the methodology is efficient to simulate Darrieus in light of the experimental data available, also to optimize a mesh grid that will be used for further analysis cases. Trend capturing by numerical results was the good by grid 4, it has almost captured the trend well. Regarding to deviation between numerical results and experimental data results, grid 3 has showed the closer matching at all TSRs as further refining did not improve the results to be closer to experimental data. Since refining the grid further than fifth grid (~700,000 element) seems not practical -as limited computational resources are available-, nor improving the results, no finer grid than grid 5 will be considered, also, grid 3 was found the best option to be used for further analysis.

### 3.8 Conclusion

As given above, grid independency test was carried out, and solution convergence was checked regarding the number of rotations. Grid 3 was found the most suitable option to proceed with in terms of relative accuracy as well the computational power requirements. Ten Revolutions were found to be enough to get a stable solution. Also, Courant number analysis has showed acceptable values range below "10" at airfoil neighbor for different azimuthal locations for grid 3. In all, this methodology applied with elements' number of about 170k was found to be consistent, and can be able to handle further analysis for a pair of Darrieus turbines.

# Chapter 4

## Results and discussion

In this chapter, we will present and discuss this study results for both cases of single and pair turbines. Firstly, full operational range of turbine will be inspected for single turbine case. Then, interaction effects between turbines in pair will be studied at different TSRs.

### 4.1 Standalone Darrieus turbine

In order to check the numerical results behavior comprehensively, simulations at a range of TSRs from 2.0 to 4.0 were carried out. Simulation inputs and methodology were followed as described in chapter 3. Figure 4.1 below presents Cp-TSR curve for numerical results achieved, compared with experimental results from [11].

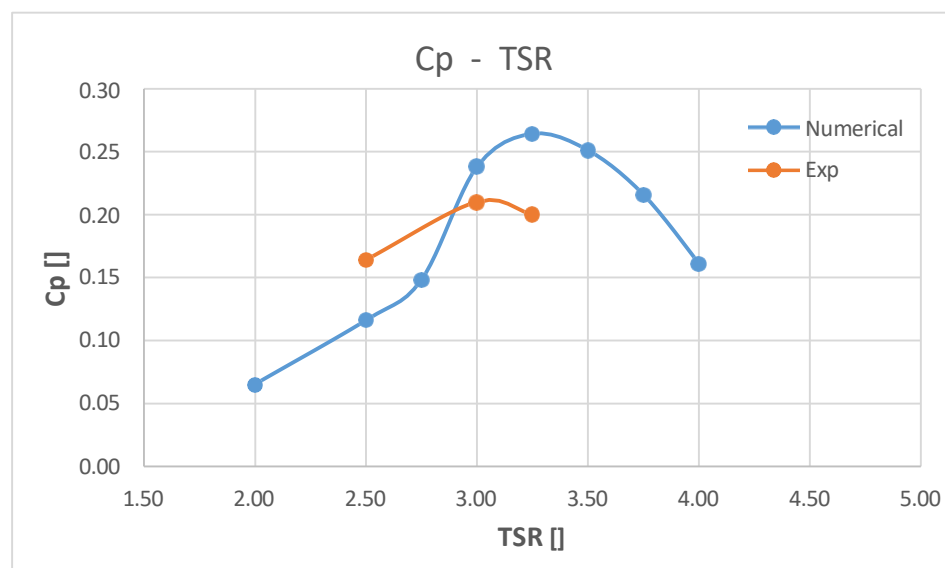


Figure 4.1: Numerical Vs Experimental results for single turbine

As shown in figure 4.1 above, numerical results have clearly overestimated the experimental results, such overestimation can be expected to exist due to the two-dimensional modelling approximation, as tip losses and parasitic losses are neglected in the 2D model. Such overestimation was also noticed in literature as reported by F. Balduzzi et. al. [15], see figure 4.2 below.

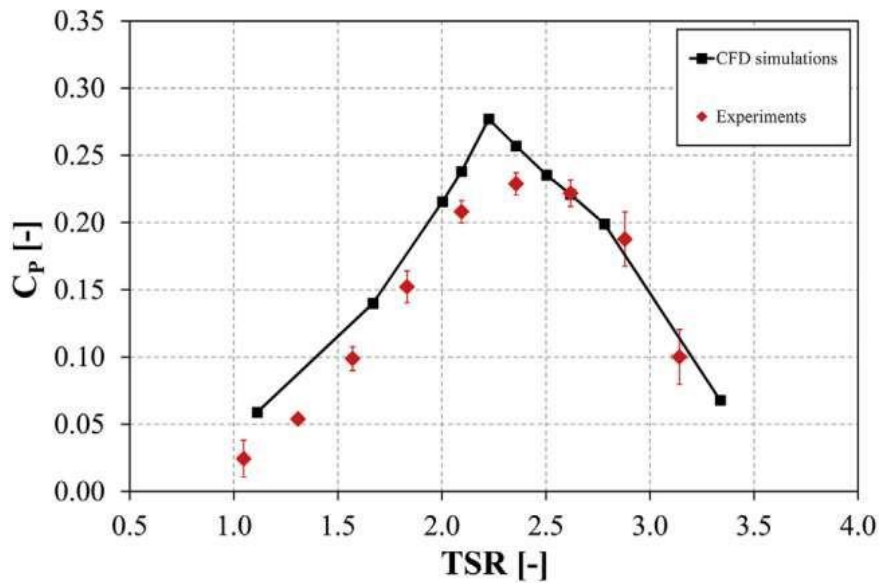


Figure 4.2: Cp vs TSR, Results of F Balduzzi et. al. [15]

Figure 4.2 shows an excellent match between experimental and numerical results; however, the overestimation percentage of the peak point was almost similar as in our results. In our study, the percentage difference between numerical to experimental peaks was 23.8 %, while the results of Balduzzi shows a percentage difference of 21%. Furthermore, a clear phase shift can be noticed between experimental and numerical results in both our results, and the results by Balduzzi. In figure 4.1, numerical results showed an optimum operation point at TSR of 3.25, while the peak of experimental results was at TSR 3.0. In Figure 4.2 also phase shift is clear, however, numerical results showed earlier peak than the experimental one. The percentage deviation of the phase shift was 8.3 % by us while it was almost 6.9% by [15]. Phase shift between numerical and experimental results can be referred the blockage effect attendance in wind tunnel, however, turbines' design and number of blades seems to play a role in the amount and the direction of the phase shift as can be noticed when comparing figures above.

## 4.2 Pair of Turbines

Many studies have focused on the effect of Darrieus turbines matching which occurs by placing rotors in a close proximity, an enhancement on the power production was reported by [11] and [17]. In the case of HAWT farms, the distance between turbines is suggested to be within 10 times of the diameter to keep proper efficiency, while the power production significantly decrease as the distance is closer. On contrast, Darrieus turbine shows ability to have better power production for closer proximity, or at least shows no significant deterioration in efficiency, which allows for better land utilization. Figure 4-3 below shows possible pairing configurations.

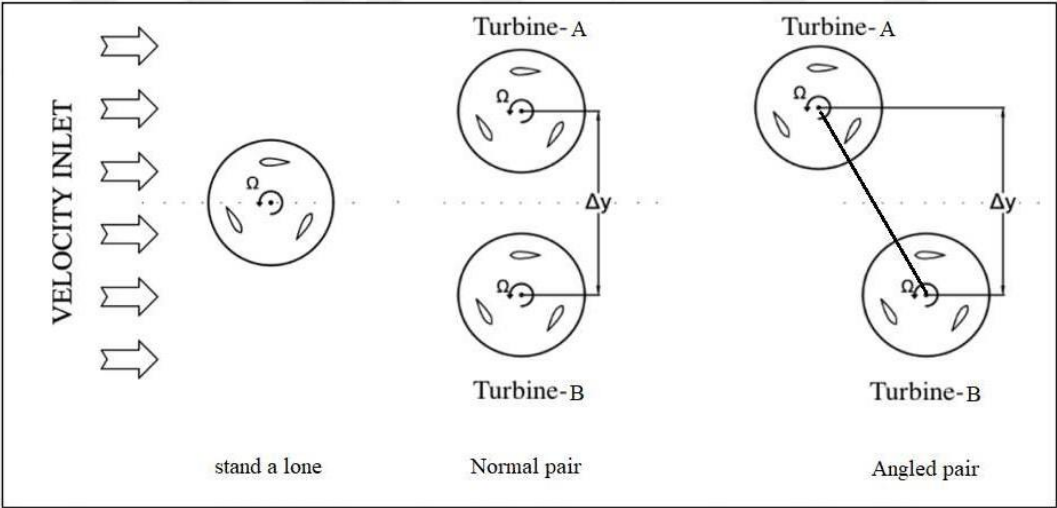


Figure 4.3: Single and pair of Darrieus turbines configurations

Center to center distance between turbines keeps playing an important role in determining how the efficiency is affected by turbines pairing, also, other factors like wind direction, and turbine’s design are attendants too. In case of standalone turbine, Darrieus machine’s performance is independent from wind direction, however, in case of turbines in pairs or arrays wind direction plays a critical role in performance efficiency due to shadowing effect. Moreover, turbines solidity, number of blades, and even mode of operation affect interaction between pair elements and resultant power production.

Figure 4.3 above shows geometrical possible arrangement for pairs configurations, while another classification based on the direction of rotation also exists. Pairs can be classified into co-rotating and counter rotating. If both turbines are rotating in same direction as the one shown in figure 4.3 then it is called co-rotating. However, the pair is called counter-rotating if each turbine is rotating in opposite direction relative to its neighbor. Additional classification is stated based on the direction of blades' motion within the region between turbines relative to wind direction. If blades are moving against wind flow direction, then it's called up-wind configuration, while it is called downwind configuration if blades are moving in same direction as wind. In our study, the pair configuration under discussion is normal to wind direction, counter rotating pair, and up-wind configuration as clarified in figure 4.4 below.

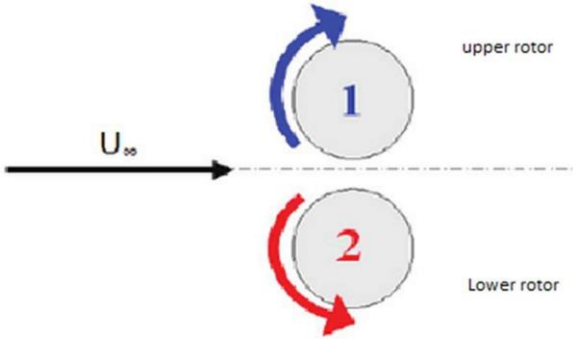


Figure 4.4: Counter rotating, upwind pair configuration

In order to represent the performance of a turbines pair compared to the stand-alone turbine; the average of both paired turbines is calculated by simply summing up the output of both, and dividing over two.

Figure 4.5 below shows results we achieved in this study as a comparison between stand-alone and pairs of turbines. All pair configurations were normal to wind direction with center-to-center distance ranges from 1.2D to 1.6D. Same procedure, as discussed in chapter 3, was followed strictly. Mesh grid 3 was used for all simulations of single and pair cases. As shown in the figure 4.5, three points were analyzed for pair turbines:

at TSR of 2.5 which represents the start-up region, TSR of 3.0 which represents pre-peak region, and at TSR of 3.5 which represents the post-peak region.

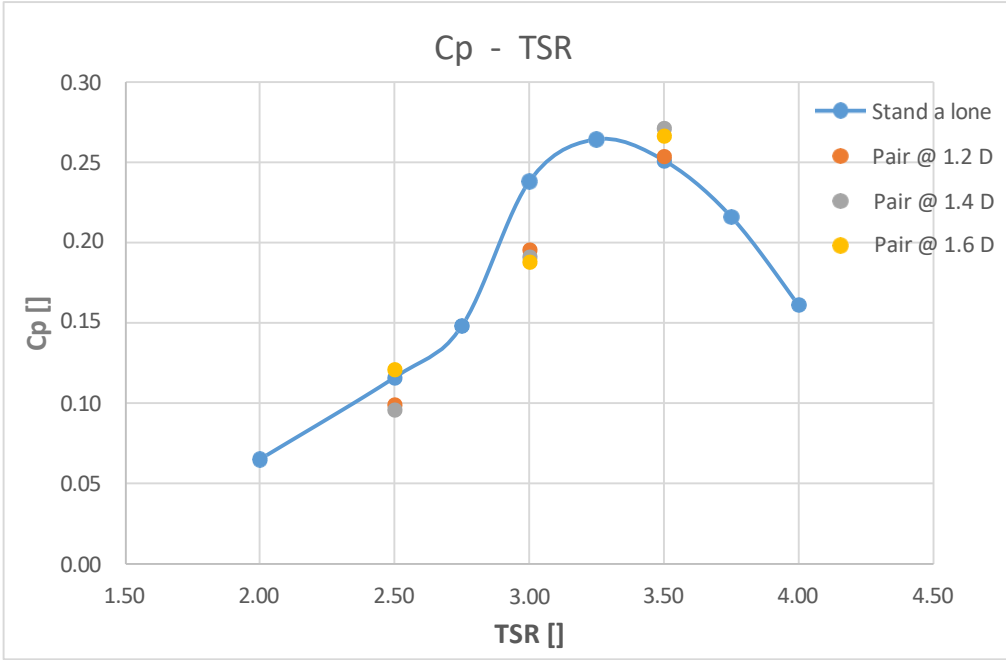


Figure 4.5: Numerical results for single and pairs of turbines

Relative to the stand-alone turbine case, turbines' pairing showed almost positive effect on average power production for TSR 3.5 specially with increasing separation distance up to 1.4D. In contrast, the performance was affected negatively by 18% at TSR 3.0, and 14% at TSR 2.5 for all pairs, except the case of 1.6D where a slight enhancement is witnessed. These results conform and assure the main assumption that Darrieus turbine offers better land utilization efficiency, such that no performance deterioration is seen, even at very close proximity of turbines locations. As Darrieus turbine should be designed to operate normally within the peak region where numerical results show performance enhancement, we can conclude that pairing will enhance the efficiency of the turbine in most of its operational period

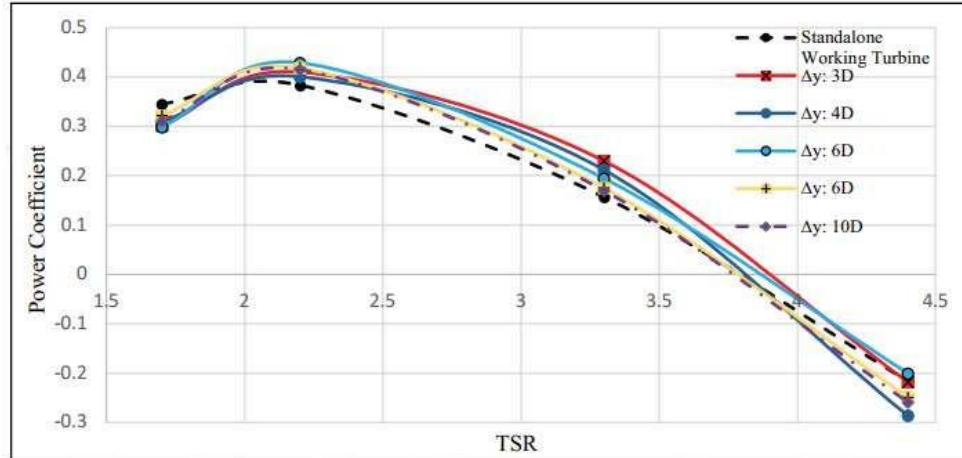


Figure 4.6: Numerical results for single and pair of turbines  $C_p$  vs TSR [21]

In order to compare our results to related literature, figure 4.6 above shows numerical results by Ö. Gencer [21] for multiple configurations of a three bladed Darrius turbines pair, compared to a stand-alone turbine. All pairs' configurations were normal to the wind direction with different separation distances of 3D, 4D, 6D, 8D, and 10D. Power production enhancement for pairs at all proximities relative to the stand-alone case can be noticed at the near post-peak region of operation. However, the simulation expected lower efficiency for pair than single turbine in the regions of operation before peak and at higher TSR far away from the optimum operation region.

Such behavior similarity between the results reported in this study and results by [21], may lead to assumption that numerical simulation face difficulties in predicting pair of turbines efficiency in the region of operation before peak, and in the region at higher TSRs exceeding the optimum region of operation. This assumption can be supported by the fact of high flow field complexity in the mentioned regions, while the flow field is more stable and more predictable in the region closely after the curve's peak.

In order to investigate numerical results more deeply, figure 4.7 shows average moment coefficient for pair of turbines at 1.2 D distance. Results of TSR 2.5, 3.0 and 3.5 are included.



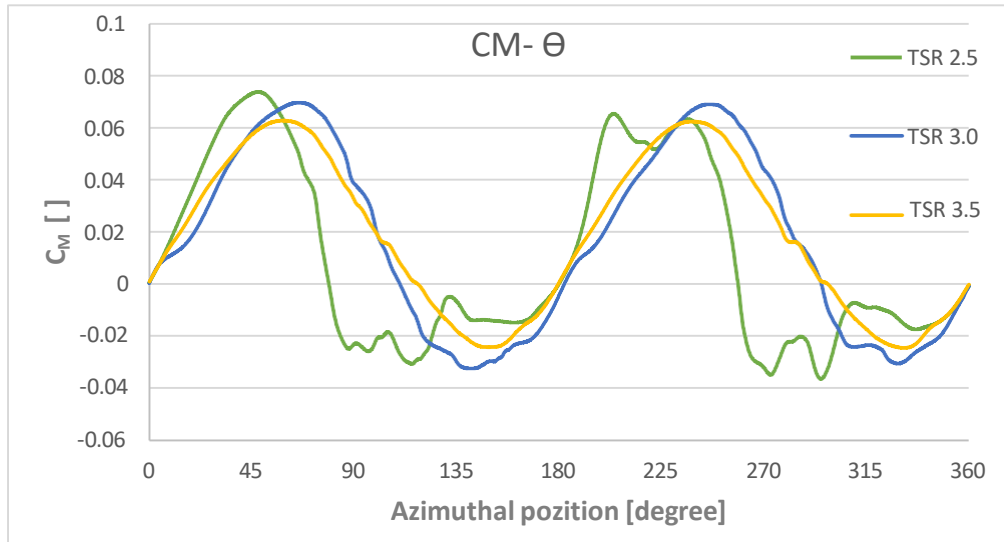


Figure 4.7: Average Moment coefficient for pair at 1.2D vs  $\Theta$ .

Since we learned that different TSRs cause different modes of operations, so the produced moment curves are expected to be significantly different. However, it can be noted that the resulted curve at TSR of 3.5 is more regular than others, and has a smaller negative component in the downturn, which can be referred to less dynamic stall effect after the performance peak point. To check out the effect of pairing on the moment curve, figure 4.8 below shows comparison for moment coefficient between the cases of single turbine and pairs of turbines at TSR of 3.0.

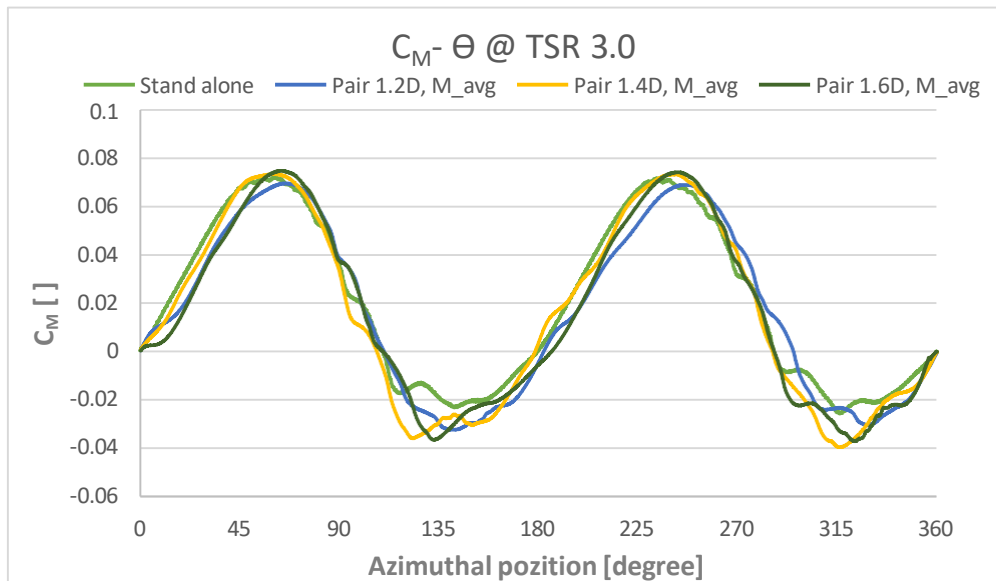


Figure 4.8: Moment Coefficient vs  $\Theta$  for stand-alone and pair configurations

Figure 4.8 above shows moment coefficient curves for single, and pairs at 1.2D, 1.4D, and 1.6D. Investigation of the pairing effect through the figure affirms that there is a clear delay phase shift by almost 10 degrees for the curve peak of pair results. Moreover, around the angles of 90 and 270, moment production of the pairs shows positive ripple, which indicates that at time blades pass next to each other, positive effect on power production is reported.

At first glance, both turbines in the pair configuration under discussion seems to have identical operation conditions, which leads to expect an identical output of both of them. However, some deviations can be noticed in moment coefficient plot of each turbine which shown in figure 4.9 below.

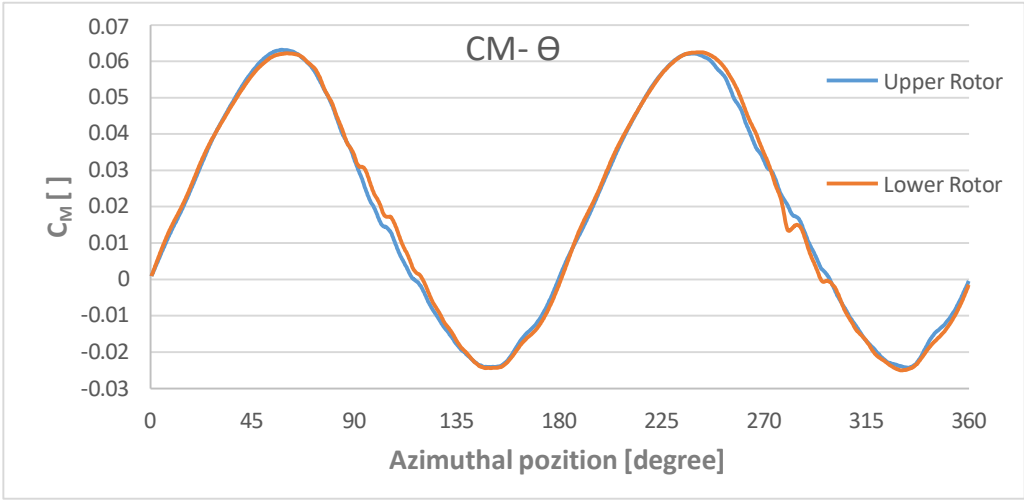


Figure 4.9: Moment coefficient for pair elements at TSR 3.5 & 1.2D

Figure 4.9 shows a comparison between the output of each turbine in a pair with 1.2D separation distance operating at TSR 3.5. As witnessed in the figure above the majority of curves deviation occurs around the azimuthal positions 90- and 270-degree angles, the angles at which blades shake hands. Even the averaged outputs of both turbines show a minimal superiority of the lower turbine in the pair, such deviations require a deeper investigation.

Figure 4.10 below illustrates the wake behavior of an isolated Darrieus turbine rotating in counterclockwise direction. It can be noticed from right-hand side of the figure, that the wake produced by Darrieus turbine tends to be directed downward making an angle with freestream wind flow direction. This behavior of Darrieus turbine's wake can justify the deviation between turbines' output in same pair which shown in figure 4.9 above. Wake field directionality depends on rotation direction and TSR as well, pair's configuration, however when a wake from a turbine affects the flow field of a turbine in neighbor, it induces additional flow turbulency which tends to enhance the performance of the latter, as a great advantage of Darrieus turbine.

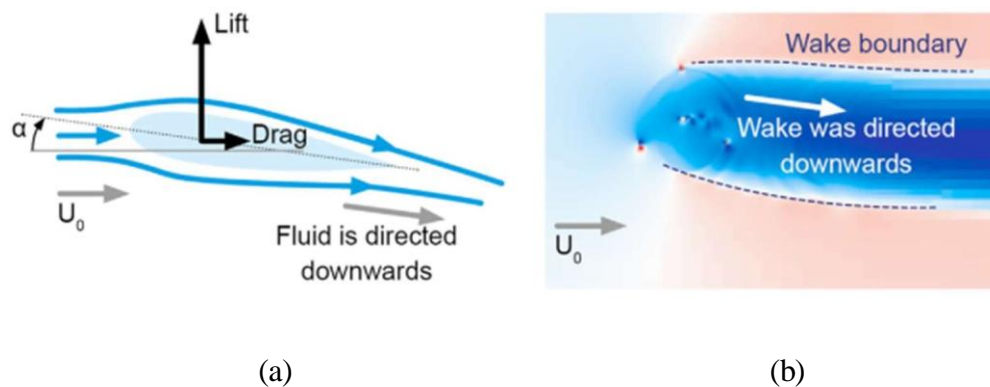


Figure 4.10, (a): Wind flow over airfoil, (b) Wake field of Darrieus turbine [17]

## 4.3 Conclusion

Due to the complex nature of flow field through Darrieus turbine, our discussed CFD results has overestimated the experimental results, However, results accuracy was noticed to be better and more reliable at higher TSR region of operation. Even though, our CFD methodology seemed to be able to handle the problem more accurately in the stable region of operation around the peak of CP-TSR curve. Solving the problem within the design conditions can be counted as an achievement, instead of seeking accurate results for full range of operation from start-up to overspeed. However, many options are available to enhance modelling accuracy for future studies such that implementing 4-equations turbulence model, using 2.5D modelling, or considering LES option.

Enhancing CFD results accuracy even seems possible, it may require huge computational resources, while in our study we tried to achieve the best possible results with implementing a personal computer's power. Based on our observations a pair of the analyzed Darrieus turbine in a wind stream flowing in normal direction to the pair, is able to keep the efficiency of power production in the same level of single turbine case, valid at close separation distance between turbines down to  $1.2D$ . Result for the pair of turbine assures what is reported previously about Darrieus turbine ability to work in pair, however we tried to support our study with experimental data. Future studies of Darrieus turbine may also discuss the effect of turbines' pairing on structural loads.

# References

- [1] IRENA, Renewable Energy Statistics 2022, International Renewable Energy Agency, Abu Dhabi; 2022.
  
- [2] Almohammadi KM, Ingham DB, Ma L, Pourkashanian M. Effect of Transitional Turbulence Modelling on a Straight Blade Vertical Axis Wind Turbine. *Advanced Structured Materials*. Springer Berlin Heidelberg; 2013. p. 93–112.  
[http://dx.doi.org/10.1007/978-3-642-40680-5\\_5](http://dx.doi.org/10.1007/978-3-642-40680-5_5)
  
- [3] Dabiri JO. Potential order-of-magnitude enhancement of wind farm power density via counter-rotating vertical-axis wind turbine arrays. Vol. 3, *Journal of Renewable and Sustainable Energy*. AIP Publishing; 2011. p. 043104.  
<http://dx.doi.org/10.1063/1.3608170>
  
- [4] Meyers J, Meneveau C. Optimal turbine spacing in fully developed wind farm boundary layers. Vol. 15, *Wind Energy*. Wiley; 2011. p. 305–17.  
<http://dx.doi.org/10.1002/we.469>
  
- [5] Whittlesey RW, Liska S, Dabiri JO. Fish schooling as a basis for vertical axis wind turbine farm design; 2010. <https://arxiv.org/abs/1002.2250>
  
- [6] Mohan Kumar P, Sivalingam K, Lim TC, Ramakrishna S, Wei H. Review on the Evolution of Darrieus Vertical Axis Wind Turbine: Large Wind Turbines. Vol. 1, *Clean Technologies*. MDPI AG; 2019. p. 205–23.  
<http://dx.doi.org/10.3390/cleantechnol1010014>

- [7] Sunyoto A, Wenehenubun F, Sutanto H. The effect of number of blades on the performance of H-Darrieus type wind turbine. 2013 International Conference on QiR. IEEE; 2013. <http://dx.doi.org/10.1109/QiR.2013.6632563>
- [8] Tjiu W, Marnoto T, Mat S, Ruslan MH, Sopian K. Darrieus vertical axis wind turbine for power generation I: Assessment of Darrieus VAWT configurations. Vol. 75, Renewable Energy. Elsevier BV; 2015. p. 50–67. <http://dx.doi.org/10.1016/j.renene.2014.09.038>
- [9] Nahas MN. A self-starting Darrieus-type windmill. Vol. 18, Energy. Elsevier BV; 1993. p. 899–906. [http://dx.doi.org/10.1016/0360-5442\(93\)90002-U](http://dx.doi.org/10.1016/0360-5442(93)90002-U)
- [10] Strickland JH. Darrieus turbine: a performance prediction model using multiple stream tubes. United States; 1975.
- [11] Vergaerde A, De Troyer T, Standaert L, Kluczevska-Bordier J, Pitance D, Immas A, et al. Experimental validation of the power enhancement of a pair of vertical-axis wind turbines. Vol. 146, Renewable Energy. Elsevier BV; 2020. p. 181–7. <http://dx.doi.org/10.1016/j.renene.2019.06.115>
- [12] Strickland JH, Webster BT, Nguyen T. A Vortex Model of the Darrieus Turbine: An Analytical and Experimental Study. Vol. 101, Journal of Fluids Engineering. ASME International; 1979. p. 500–5. <http://dx.doi.org/10.1115/1.3449018>
- [13] Blackwell BF, Sheldahl RE, Feltz LV. Wind tunnel performance data for the Darrieus wind turbine with NACA 0012 blades. Office of Scientific and Technical Information (OSTI); 1976 May. <http://dx.doi.org/10.2172/7269797>
- [14] Bianchini A, Balduzzi F, Rainbird JM, Peiro J, Graham JMR, Ferrara G, et al. An Experimental and Numerical Assessment of Airfoil Polars for Use in Darrieus Wind Turbines—Part I: Flow Curvature Effects. Vol. 138, Journal of

Engineering for Gas Turbines and Power. ASME International; 2015.  
<http://dx.doi.org/10.1115/1.4031269>

- [15] Balduzzi F, Bianchini A, Maleci R, Ferrara G, Ferrari L. Critical issues in the CFD simulation of Darrieus wind turbines. Vol. 85, Renewable Energy. Elsevier BV; 2016. p. 419–35. <http://dx.doi.org/10.1016/j.renene.2015.06.048>
  
- [16] Barnes A, Marshall-Cross D, Hughes BR. Towards a standard approach for future Vertical Axis Wind Turbine aerodynamics research and development. Vol. 148, Renewable and Sustainable Energy Reviews. Elsevier BV; 2021. p. 111221. <http://dx.doi.org/10.1016/j.rser.2021.111221>
  
- [17] Hansen JT, Mahak M, Tzanakis I. Numerical modelling and optimization of vertical axis wind turbine pairs: A scale up approach. Vol. 171, Renewable Energy. Elsevier BV; 2021. p. 1371–81.  
<http://dx.doi.org/10.1016/j.renene.2021.03.001>
  
- [18] Darrieus G. Turbine Having Its Rotating Shaft Transverse to the Flow of the Current. U.S. Patent 1835018. 8 December 1931.
  
- [19] Batista N, Melicio R, Mendes V, et al. Darrieus-type vertical axis rotary-wings with a new design approach grounded in double-multiple stream tube performance prediction model. Vol. 6, AIMS Energy. American Institute of Mathematical Sciences (AIMS); 2018. p. 673–94.  
<http://dx.doi.org/10.3934/energy.2018.5.673>
  
- [20] Han Y, Sitaraman J, Dan Y. Analysis of vertical axis wind turbine aerodynamics by using a multi-fidelity approach. Annual Forum Proceedings - AHS International. 3. 2101-2111; 2014

- [21] Gencer Ö. Energy interaction of vertical axis wind turbines working in pairs. Master's thesis- Izmir Institute of technology; March 2023.
- [22] Yuan Z, Jiang J, Zang J, Sheng Q, Sun K, Zhang X, et al. A Fast Two-Dimensional Numerical Method for the Wake Simulation of a Vertical Axis Wind Turbine. Vol. 14, *Energies*. MDPI AG; 2020. p. 49.  
<http://dx.doi.org/10.3390/en14010049>
- [23] Duraisamy K, Lakshminarayan V. Flow Physics and Performance of Vertical Axis Wind Turbine Arrays. 32nd AIAA Applied Aerodynamics Conference. American Institute of Aeronautics and Astronautics; 2014.  
<http://dx.doi.org/10.2514/6.2014-3139>
- [24] Chakoua P, Wamkeue R, Ouhrouche M, Tameghe T, Ekemb G. A New Approach for Modeling Darrieus-Type Vertical Axis Wind Turbine Rotors Using Electrical Equivalent Circuit Analogy: Basis of Theoretical Formulations and Model Development. Vol. 8, *Energies*. MDPI AG; 2015. p. 10684–717.  
<http://dx.doi.org/10.3390/en81010684>
- [25] Bremseth J, Duraisamy K. Computational analysis of vertical axis wind turbine arrays. Vol. 30, *Theoretical and Computational Fluid Dynamics*. Springer Science and Business Media LLC; 2016. p. 387–401.  
<http://dx.doi.org/10.1007/s00162-016-0384-y>
- [26] Scheurich F, Brown RE. Modelling the aerodynamics of vertical-axis wind turbines in unsteady wind conditions. Vol. 16, *Wind Energy*. Wiley; 2012. p. 91–107. <http://dx.doi.org/10.1002/we.532>
- [27] Paraschivoiu I. Wind turbine design with emphasis on Darrieus concept. Montreal: Polytechnique International Press; 2002.
- [28] Rogowski K, Hansen MOL, Lichota P. 2-D CFD Computations of the Two-Bladed Darrieus-Type Wind Turbine. Vol. 11, *Journal of Applied Fluid*



Mechanics. Academic World Research; 2018. p. 835–45.

<http://dx.doi.org/10.29252/jafm.11.04.28383>

- [29] Sørensen JN, Mikkelsen RF, Henningson DS, Ivanell S, Sarmast S, Andersen SJ. Simulation of wind turbine wakes using the actuator line technique. Vol. 373, Philosophical Transactions of the Royal Society A: Mathematical, Physical and Engineering Sciences. The Royal Society; 2015. p. 20140071.

<http://dx.doi.org/10.1098/rsta.2014.0071>

- [30] Łukaszewicz G, Kalita P. Navier–Stokes Equations. Advances in Mechanics and Mathematics. Springer International Publishing; 2016.

<http://dx.doi.org/10.1007/978-3-319-27760-8>

- [31] Menter FR. Two-equation eddy-viscosity turbulence models for engineering applications. Vol. 32, AIAA Journal. American Institute of Aeronautics and Astronautics (AIAA); 1994. p. 1598–605. <http://dx.doi.org/10.2514/3.12149>

- [32] Inflation Layers / Prism Layers in CFD [Internet]. United Kingdom; 2021 June 24 [cited 2023 November 5]. Video: 47:13 min. Available from:

<https://www.youtube.com/watch?v=1gSHN99I7L4&list=PLnJ8IIgfDbkqaOdo-twtuco-qYahdAeG8>

- [33] Mauro S, Brusca S, Lanzafame R, Messina M. Micro H-Darrieus wind turbines: CFD modeling and experimental validation. SECOND INTERNATIONAL CONFERENCE ON MATERIAL SCIENCE, SMART STRUCTURES AND APPLICATIONS: ICMSS-2019. AIP Publishing; 2019.

<http://dx.doi.org/10.1063/1.5138842>

- [34] Zanforlin S, Nishino T. Fluid dynamic mechanisms of enhanced power generation by closely spaced vertical axis wind turbines. Vol. 99, Renewable Energy. Elsevier BV; 2016. p. 1213–26.

<http://dx.doi.org/10.1016/j.renene.2016.08.015>

- [35] Balduzzi F, Bianchini A, Ferrara G, Ferrari L. Dimensionless numbers for the assessment of mesh and timestep requirements in CFD simulations of Darrieus wind turbines. Vol. 97, Energy. Elsevier BV; 2016. p. 246–61.  
<http://dx.doi.org/10.1016/j.energy.2015.12.111>
- [36] Trivellato F, Raciti Castelli M. On the Courant–Friedrichs–Lewy criterion of rotating grids in 2D vertical-axis wind turbine analysis. Vol. 62, Renewable Energy. Elsevier BV; 2014. p. 53–62.  
<http://dx.doi.org/10.1016/j.renene.2013.06.022>
- [37] Mojtaba A. Analysis and Improvement of Aerodynamic Performance of Straight Bladed Vertical Axis Wind Turbines. Ontario, Canada: University of Windsor; 2015. Available From. <https://scholar.uwindsor.ca/etd/5625>

## Eng. ABDELRAHMAN ABULEENEIN

### Education:

- High school Certificate, **Hunein High School**, Amman, 2011, Scientific Stream, (95.2%)
- BSc in Mechanical Engineering, **University of Jordan**, Amman, 2015, (GPA 3.31 out of 4)
- English proficiency test (**IELTS**), Academic Branch, 6.5 out of 9, 2018
- Masters in Energy Engineering, **Izmir Kâtip Çelebi University**, In Progress

### Work Experience:

- Mechanical Design, and site Engineer, **IRIS for Manufacturing Technology Co.** Amman-Jordan, 2015 to 2017
- Mechanical Engineer, Technical Support Dept. **PETRA Engineering Industries Co.** Amman-Jordan, 2017 to 2019
- Procurements Officer, Technical Support Dept. **Mohammad Eisa Trading Co.** Amman-Jordan, Online Based Job, 2019 to 2020.

### **Under-Graduation Project**

Simulate the impact of a 7.62 mm Projectile into Steel Plate, this work aimed to find the steel response against impact loading and the minimum thickness of hard 4340 steel and armox steel that can stop the projectile with suitable factor of safety, the major work was in introducing the modern simulation techniques which minimize analysis cost and save time Dramatically, as well this work supplied us with ability to analyze different structure and machines for static and dynamics loads using numerical methods.